RESEARCH ARTICLE

European Journal of
Lipid Science and Technology
www.ejlst.com

Influence of Minor Oil Components on Sunflower, Rice Bran, Candelilla, and Beeswax Oleogels

Maria Scharfe, Jonas Niksch, and Eckhard Flöter*

The impact of the solvent composition on wax oleogels is addressed by (1) increasing polar components (PC) in sunflower and canola oil through thermal treatment and (2) removing minor components from untreated oils by column chromatography. Subsequently, oleogels are produced at 0.05 and 10 °C min^{-1} using 4% or 10% w/w of either sunflower, rice bran, candelilla, or beeswax. Oleogels firmness, break-up behavior during amplitude sweeps, and gelation and dissolution are studied using penetration tests, rheology, and differential scanning calorimetry (DSC), respectively. Moreover, the crystal morphology of 4% w/w samples, gelled at 10 and 0.05 °C min^{-1}, is studied using bright field microscopy. Distinct effects caused by the presence or absence of PCs on the characteristics mentioned above are observed, depending on the wax type. The formation of highly ordered wax crystal structures is favored in oils without PCs and low cooling rates. Data on gel formation and dissolution reveal a decrease in wax solubility in the absence of PCs. In contrast, the critical gelation concentration (CGC) decreases when PCs are present, independent of their concentration, indicating that PCs aid network formation. Moreover, the break-up behavior during oscillatory stress is significantly different, leading to more network fragments and higher energy dissipation with increasing strain.

***Practical applications*: It is found that the oil composition, in particular, the fatty acid composition of TAGs and dissolved minor polar oil components, profoundly affect wax oleogel properties. Although not all mechanisms leading to these changes can be unraveled within this study, a fundamental understanding of solvent composition's role on oleogel formation, dissolution, and network properties is vital in the light of product applications. Moreover, trustworthy and comparable oleogel research can only be achieved if the impact of solvent composition is considered in experiments. That way, the capability of oleogels for industrial applications might be maximized. For that, a detailed characterization of oil quality, particularly the fatty acid composition and presence of minor polar components, is required to conduct reliable scientific work in oleogel research.**

1. Introduction

Waxes are organic, lipophilic mixtures of long alkyl chains having several functional groups such as carboxyl, hydroxyl, ketones, aldehydes, and esters. Additionally, the chains may comprise unsaturated bonds. Hence, plant waxes contain a heterogeneous mixture of wax esters (WEs), free fatty acids (FFAs), fatty alcohols (FAOHs), hydrocarbons (HCs), and up to 10% other minor components.[1] The chemical composition, e.g., alkyl chain length and number of unsaturated bonds, and the ratio of these components defines the waxes' physicochemical characteristics such as dissolution temperature (T_D) and solubility in a particular solvent.

The composition considerably depends on the wax source, growing conditions, and extraction and purification methods indicated by the compositional differences found in the literature.[1–11] Besides the main constituents, minor wax components such as sterol esters, esters of pentacyclic triterpenoids, and alcohols and their concentration may influence, i.a., transition temperatures.[12] However, in their native state, waxes are solid at ambient temperature and usually melt between 50 and 80 °C.[13]

When dissolved in low polar, organic solvents such as edible oils at sufficient concentrations, they may form a 3D crystalline network that can immobilize the liquid (see **Table 1**). The resulting oleogels are promising candidates to replace traditionally structured lipid phases based on semi-solid networks with high saturated fatty acids contents.

Waxes of industrial significance are beeswax (BWX), carnauba (CRX), candelilla (CLX), rice bran (RBX), and sunflower wax (SFX). The ability of waxes to gel, e.g., plant oils, relates to their low solubility and crystal structure, which is a function of their

The ORCID identification number(s) for the author(s) of this article can be found under https://doi.org/10.1002/ejlt.202100068

DOI: 10.1002/ejlt.202100068

M. Scharfe, J. Niksch, E. Flöter
Department of Food Processing
Technical University Berlin
Berlin 13353, Germany
E-mail: maria.scharfe@tu-berlin.de

Table 1. Selection of literature, including the CGC determination of SFX, RBX, CLX, and BWX in different oils. The list does not aim to cover all publications measuring the CGC of waxes in edible oils. Values were determined at ambient temperature (20 or 25 °C), except.[50]

Wax	CGC [% w/w]	Δ% w/w	Oil	Method	Ref.
SFX	0.5	0.5	Soybean	Flow test	[7]
	1.0	1.0	Canola	Flow test	[3]
	0.5	0.5	High oleic sunflower	Flow test +Rheology	[50]
	1.0	0.5	Rice bran	Flow test	[26]
	0.3, 0.5 &1.0	0.2, 0.5, and 1.0	Soybean, almond, canola, corn, grape seed, safflower & sunflower (all 0.3) olive, peanut, pumpkin, sesame, and walnut (all 0.5), flaxseed (1.0)	Flow test	[51]
RBX	1.0	0.5 and 1.0	Olive oil	Flow test	[5]
	1.0	1.0	Canola	Flow test	[3]
	5.0	2.0	Rice bran	Flow test	[52]
	5.0	0.5	Rice bran	Flow test	[26]
CLX	2.0	0.5 and 1.0	Refined soybean	Flow test	[53]
	2.0	0.5 and 1.0	Olive oil	Flow test	[5]
	1.0-2.0	0.5	Soybean	Flow test	[7]
	2.0	1.0	Canola	Flow test	[3]
	0.75	0.25	High oleic sunflower	Flow test	[50]
	1.0	0.5	Rice bran	Flow test	[26]
BWX	2.0–3.0	0.5	Soybean	Flow test	[7]
	1.0	0.25	High oleic sunflower	Flow test+ Rheology	[50]
	4.0, 4.0	2	MCT, LCT	Flow test	[52]
	1.5	0.5	Rice bran	Flow test	[26]

chemical composition and the interactions between individual components and the gels' production conditions, such as cooling rate and shear. Moreover, the solvent composition and dissolved PCs could impact the gelling ability of waxes by interacting with the main wax components or modifying the network-defining interactions between the crystals. Similar effects have been reported for interactions in fat crystal networks in the presence of molecules with functional groups.[14–17]

Hence, the main wax components and potential interaction points will be discussed briefly in the following. Hydrocarbons with odd and even-numbered alkyl chains (27–36) self-assemble into lamellar structures, forming crystalline microplatelets in hydrophobic solvents. These aggregate and form a 3D network stabilized by mainly van der Waals forces (vdW).[18] The melting temperature increases with increasing carbon chain length, simultaneously decreasing the solubility.[19] That applies to all wax constituents.

Combinations of long-chain FFAs and FAOHs reportedly gel vegetable oils at concentrations as low as 2% w/w and show synergistic effects at specific composition ratios when having the same chain length.[20] In addition, due to their carboxylic group, hydrogen bonds form during the self-assembling process resulting in stronger network interactions than HCs. These bonds reportedly boost interactions in other oleogels systems as well.[21] Consequently, their melting temperatures are higher than HCs with the same number of carbon atoms.[20] Natural waxes contain FAOHs with even-numbered carbon chains between 24–34 carbon atoms.[22] Their weight fraction in waxes ranges from less than 1% in RBX and SFX, 2 and 6% in BWX and CLX, to more than 30% in CRX. Similar to FFAs strong hydrogen bonds form between adjacent FAOHs through their hydroxyl groups.

Finally, wax esters are the main components in SFX, RBX, BWX, and CRX, possibly impacting oleogel formation and properties the most. They contain FA and FAOH moieties with carbon chain lengths between 16–24 and 18–31, respectively.[22] The proportion of the two alkyl chains in WE's influences the phase transition, with symmetric WE showing higher melting temperatures.[23,24] The self-assembly of WE is due to the interlocking of alkyl chains which is more favored if adjacent chains have the same number of carbon atoms.[25] These structural units form large plates of stacked crystals (symmetrical), while asymmetric chains result in smaller, more needle-like shapes.[23]

Besides processing conditions and wax composition, weak, noncovalent bonds between crystals such as hydrogen bonds, vdW forces, and π–π-interactions additionally impact network strength.[6,26,27] These may form by bridging between adjacent crystals. Moreover, minor oil and wax components alter crystallization kinetics and crystal morphologies. Indeed, a study showed that minor wax components with functional groups such as secondary alcohols or ketones do not develop the orthorhombic structure typical for aliphatic compounds. That results from reduced crystallinity which favors more loosely mixed molecular packing.[3] Therefore, minor components may profoundly affect crystal morphology, changing macroscopic properties such as gel hardness. Possible effects due to minor oil and wax components' are difficult to assess. The more so because of the chemical diversity and varying concentrations.

Nevertheless, several publications addressed the role of oil type on wax oleogels. The rheological and thermal behavior of SFX, BWX, and paraffin wax (PFX, only HCs: C20+C40) was studied in olive, corn, soybean, sunflower, safflower, and canola oil.[28] Dissolution temperatures (T_D) and transition enthalpies were affected by the oil type, whereas the degree of change differed for all waxes. Similarly, the storage modulus, which represents the number of interaction points within a network,[31] showed considerable differences in oil and wax types. Another study assessed the crystallization of RBX in a canola/soybean oil mix, camellia oil, and olive oil.[29] While the gel formation temperature (T_F) was not significantly affected, T_D varied slightly with the oil type, indicating minor changes in wax solubility. In line with that, penetration hardness was affected by the oil type. However, X-ray diffraction (XRD) patterns revealed two RBX crystal types and anisotropic crystal growth, resulting in needle-like crystals.

In addition to varying the oil type, adding small molecules with functional groups is a popular method to tailor also wax oleogel properties.[30,31] However, without standardization of the solvent, the effects of minor oil components and admixed molecular species are challenging to unravel due to superimposition.

The admixing of adipic acid (2 carboxyl groups, $T_m \approx 151$ °C) to CRX/soybean oil oleogels resulted in hydrogen bond formation visible in FTIR spectra.[32] These may form between the carboxyl groups of the acid and FFAs (84–85%) of CRX. Furthermore, XRD revealed modifications in the crystallinity in oleogels with adipic acid manifested in fibrillar instead of needle-like crystals.

Similarly, combining CLX with different concentrations of either monoglyceride (MAG, C18, C22) and fully hydrogenated crambe oil (FHCO, C22, C18) in high oleic sunflower oil (7% saturated FAs) and soybean oil (16% saturated FAs) altered oleogel properties.[33] Although in DSC thermograms, an increase of transition enthalpy and T_D is visible at high MAG and FHCO concentrations, this does not involve an equal increase in gel hardness. Instead, gel firmness dropped to about 20% of the initial value of CLX oleogels. The gel hardness increased by increasing the additive concentration further due to the formation of individual networks by FHCO or MAGs.

In contrast, tripalmitate (PPP) addition leads to a synergistic effect in CLX oleogels.[34] Here, systems with 1% CLX and up to 1% PPP showed higher G' than 3% CLX oleogels. Reportedly, that is due to the cocrystallization of PPP and CLX.

However, all studies considered utilized oils from supermarkets without detailed characterization of, e.g., unknown levels of minor polar components, FA profile, or viscosity. The standardization of oils is recommended to avoid the superimposition of several effects contributing to the modifications of oleogels.[21,35–37] To the best of our knowledge, only one study included an oil purification procedure to remove minor oil components before preparing SFX oleogels.[38] Different soybean oils with varying iodine values (112, 136, and 159) and PC levels (7.5%, 6.2%, 2.8%, and stripped) were used, exemplifying different oil polarities. The absence of PC increased the transition enthalpies, indicating more crystalline material. Since the enthalpy was highest for the most polar oil (highest IV), one could assume that SFX is less soluble in more polar oils. However, the purification did not affect gel firmness, but G' decreased in all stripped samples compared to natural oils.

Secondary wax and oil components containing functional groups may cause interactions with wax constituents. These might interfere with molecular stacking during gel formation, modify wax solubility, and promote mixed molecular packing formation.[3,39] In addition to wax and oil composition, the processing conditions such as cooling rate, application of mechanical forces, and storage time essentially affect wax oleogels.[2,12,22] Nevertheless, these factors have been discussed in recent literature and will be kept constant in this study. However, distinct effects influencing wax oleogel properties were reported in the literature. Since these superimpose in non-standardized oils comprising PCs, it is impossible to disentangle individual contributions. Thus, the utilization of stripped oils offers a more holistic approach.

This study aims to provide a more coherent and relevant approach to describe the impact of solvent composition (PC and TAG composition) on wax oleogels. To this end, canola and sunflower oil with varying concentrations of PC (0–19.4%) are used to produce wax oleogels utilizing SFX, RBX, CLX, and BWX. Subsequently, the gel hardness, crystal morphology, rheological and thermal properties, and CGC are analyzed. The latter was determined at 20 °C using a rheological approach with minimal concentration steps (0.05% w/w). Finally, an attempt is made to link the data on solvent composition to the microscopic and macroscopic properties of different wax oleogels, considering the individual wax compositions. That hopefully enables a better understanding of the composition-functionality relation of wax oleogels and provides new insights into the impact of PC on the formation and properties of wax crystal networks in edible oils.

2. Experimental Section

2.1. Material

BWX, CLX, SFX, and RBX were kindly provided by KAHL G.m.b.H. & Co. K.G., Trittau, Germany. The waxes were stored in plastic bags at 6 °C. Canola oil (Canolin 10 770,) and sunflower oil (Sonnin 70 020) were kindly provided by Walter Rau AG, Neuss, Germany. All oils were stored in opaque containers at 3 °C immediately after delivery to prevent deteriorating reactions.

2.2. Oil Purification and Increment of Polar Oil Components

Untreated canola, sunflower, and flaxseed oil were stripped by combining the official method for the determination of polar compounds and two methods developed in previous studies [DGF C-III 3b (13)].[40,41] The details can be found elsewhere.[35]

Sunflower and canola oil (2 l each) were heated to 180 °C and vigorously stirred to induce oil deterioration and increase the content of polar components. Samples were taken from the batch, cooled to ambient temperature, and stored at 5 °C in opaque containers. Samples were taken when the initial PC value determined using Testo 270 cooking oil tester (Titisee-Neustadt, Germany) increased by 0.5%, 1.0%, 2.5%, and 15.0% from the initial Testo value, which was 5.0% for canola and 9.0% for sunflower oil. That way, several stages of oil deterioration were reached. It should be mentioned that natural sunflower oil did not actually

contain 9.0% of total polar components. The Testo cooking oil tester measures the permittivity of a liquid and correlates the value to a reference oil. This reference oil has a lower iodine value (IV) than sunflower oil. Therefore, more unsaturated bonds result in a higher permittivity. The measured values thus overshoot the actual PC value. The value of 3.7 ± 0.2 verified this according to the official method (DGF, C-III 3b (13)).

It should be mentioned that the same oils (natural, stripped, and with increased levels of polar components) were used in previous studies. Data on the effectiveness of the oil purification procedure will hence not be shown in this study. For further information, refer to refs. [35, 42].

Except for oil analysis and oleogel firmness, only stripped and untreated oils and oils with the highest level of deterioration products were used for further analysis. They will be referred to as –P, –N, and –D, respectively.

2.3. Oil Analysis

Dielectric Constant: A parallel plate type electrode was built with two stainless steel plates. The plates were fixed at a constant distance of 0.5 mm by 4 PTFE washers (Ø 4 mm) and suitable PTFE screws (12 mm in length). Each plate was equipped with a 150 mm stranded wire (cross-sectional area 1.5 mm^2) and connected to a precision LCR meter (4280A, Hewlett Packard). The capacitor was placed in a sealed PTFE housing filled with the respective oil. The setup and the oil samples were tempered at 20 °C before analysis to ensure a constant and evenly distributed temperature, and the temperature varied less than 0.5 °C during measurements. The dielectric constant (ϵ) was determined by dividing the capacitance of the oil (C_x) by the capacitance of the air (C_0)

$$\varepsilon = \frac{C_x}{C_0} \tag{1}$$

All measurements were performed at 1 MHz and carried out in triplicates.

Total Polar Components: In addition to the Testo cooking oil tester, the content of polar components was determined using the official method employing column chromatography.[43] Briefly, 25 g silica (0.063-0.2 mm, VWR International, Pennsylvania, USA) with a water content if 5 g/100g is added to a mixture of diethyl ether (13% v/v) and petrol ether (87% v/v) (both HPLC grade and purchased from VWR International, Pennsylvania, USA) and filled into a chromatography column (21 mm inner diameter, length 45 cm, Lenz Laborglas GmbH, Berlin, Germany). Subsequently, 2.5 g of oil was weighed and dissolved in 50 mL of the solvent mixture. 20 mL of the oil solvent mixture were transferred into the column and eluted using another 150 mL of the solvent mixture. The elution time was 60–70 min, and the samples were collected in a dried flask. Once elution was completed, the solvent was evaporated at 50 °C using a vacuum rotary evaporator (600 mbar). The content of polar components can be calculated from the initial mass of the oil sample and the eluted mass collected in the flask. Measurements were carried out in triplicates.

Peroxide Value, and Free Fatty Acids: Free fatty acids (FFA) and peroxide value (PV) of oil samples were determined by titration (Excellence T5, Mettler Toledo, Columbus, USA). The PV was determined according to DGF method C-VI 6a Part 2(02) (Wheeler method). 3–5 g oil was diluted in a mixture of chloroform and acetic acid (3:2 v/v, AppliChem GmbH, Darmstadt, Germany). Subsequently, 1 mL of saturated potassium iodate (GPR RECTAPUR, VWR International, Pennsylvania, USA) solution was added. After stirring at 300 rpm for 180 s, 50 mL of deionized water were added. The titration was performed with 10.0 mol^{-1} sodium thiosulfate (Alfa Aesar, Haverhill, USA) and a redox electrode (DMi140-SC, Mettler Toledo, Columbus, USA).

The content of FFAs, expressed as oleic acid content in mg/100 g, was determined according to DGF method C-III 4 (06) with a pH electrode (DG113-SC, Mettler Toledo, Columbus, USA). Briefly, 2–4 g of oil was dissolved in 60 mL of an ethanol/diethyl ether solution (1:1 v/v, both HPLC-grade, VWR International, Pennsylvania, USA). The titration was performed using potassium hydroxide (GPR RECTAPUR, VWR International Pennsylvania, USA) in ethanol (0.02 mol/l). A blank value was determined for each new batch of solvent. The titer was determined by dissolving 25 mg benzoic acid (GPR RECTAPUR, VWR International Pennsylvania, USA) in the solvent and was measured in triplicates every day. All measurements were carried out in triplicates.

2.4. Oleogels

Gel Preparation: 200 mL stock solutions of 4, and 10% w/w wax in oil were prepared by adding the solids to the oil and heating the mixture in 400 mL glass beakers to 80 °C on a heating plate (MR Hei-Tech, Heidolph Instruments GmbH & Co.KG, Schwabach) agitated using a magnetic stirrer at 200 rpm. Before further processing, the solution was kept at 80 °C for 20 min to ensure complete dissolution.

For rheology and microscopy, hot wax solutions were directly transferred into the respective measurement environment to avoid any changes in the gels due to sample preparation and transfer. Three individual stock solutions were prepared for each oil, and measurements were repeated as described in the following sections.

Gel Firmness: Freshly prepared 10% w/w stock solutions were poured into preheated (60 °C) glass Petri dishes (Ø 110 mm) up to a height of 13 mm (50 g ±1 g). Samples were transferred into a programmable climate chamber (HPP260, Memmert GmbH, Schwabach, Deutschland) and cooled to 20 °C at a constant cooling rate of 10 or 0.05 °C min^{-1}. Subsequently, the samples were stored at the same temperature for 24 h before firmness was measured using a static material testing machine (Zwick GmbH & Co. KG, Germany) equipped with a 0.5-inch cylindrical probe. When the preset force of 0.02 N was detected, the cylinder penetrated the sample to a depth of 3 mm (<30% of sample height), and the associated program testExpertII recorded the force–displacement motion curves. Each Petri dish was penetrated five times, and the distance between penetration points and the wall of the petri dish was about 10 mm.

Gel–Sol Transition: DSC was performed using a Netzsch 204 Polyma (Netzsch-Gerätebau GmbH, Selb, Germany). Pure waxes and oleogels comprising 4% and 10% w/w wax were gelled at ambient temperature and stored for 24 h. Subsequently,

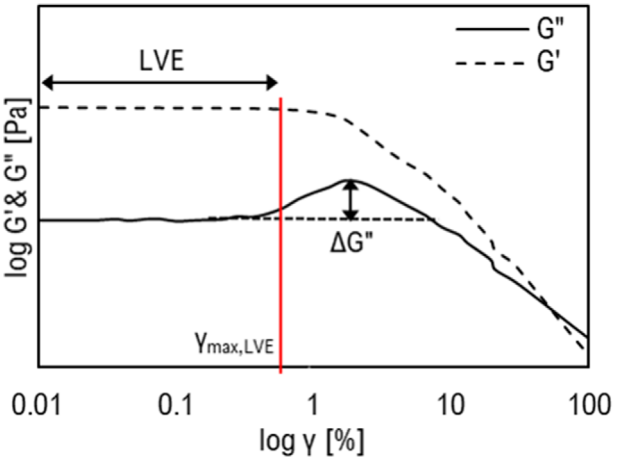

Figure 1. Exemplary plot of storage and loss modulus of wax oleogels during amplitude sweep, explanation in the text.

10–20 mg were cut from the gel samples' center, weighed into aluminum pans, and hermetically sealed. Samples were kept at 95 °C for 30 min in the calorimeter to erase crystal memory. Samples were then cooled at constant rates of 1, 10, and 40 °C min^{-1}. After an isothermal period of 20 min at 20 °C, samples were heated at 10 °C min^{-1} and the gel–sol transition temperatures and enthalpies were determined using Proteus software (Netzsch-Gerätebau GmbH, Selb, Germany). The measurements were carried out in duplicates.

Sol–Gel Transition and Viscoelastic Behavior: Sol–gel transition temperatures were determined via dynamic mechanical thermal analysis (DMTA) using an MCR 302 Rheometer (Anton Paar GmbH, Austria) with a plate-plate geometry (gap 0.2 mm). The upper plate was sandblasted to avoid slipping of the sample. Hot wax solutions (10% w/w) were pipetted (preheated pipette tips, 0.8 mL) onto the preheated plate (90 °C). Subsequently, the solution was cooled from 90 to 10 °C at a fixed cooling rate of 10 °C min^{-1}. The measurements were performed at a constant strain within the linear viscoelastic region (LVR) of both the liquid and the solid (0.05%) and an angular frequency of 10 rad s^{-1}. The sol–gel transition temperature was calculated using the associated program (Rheoplus, Anton Paar, Austria). It is defined as the crossover of the loss (G'') and storage modulus (G') upon cooling. All measurements were carried out in triplicates.

After gelation occurred, the samples were left to rest for 20 min at 20 °C. Then, a strain sweep from 0.01–100% was performed at 10 rad s^{-1} and 20 °C. The data was used to determine G''_{max} within the LVR and the strain at which the sample starts to be irreversibly damaged (γ_{max}). The threshold value for determining γ_{max} was set to 5% of the G''_{max} in agreement with the literature.[44] Moreover, $\Delta G''$ was determined by deducting G'' within the LVR from G''_{max} (see **Figure 1**).

CGC: The CGC in this study was determined for all waxes in combination with stripped, untreated, and deteriorated oils (PC +10%). It refers to the concentration at which G' exceeds G'' at 20 °C. To this end, the CGC was approximated in a first step by measuring the sol–gel transition temperature of wax solutions with varying concentrations. Subsequently, the results were plotted and extrapolated to estimate the CGC at 20 °C. The approximation of the precise CGC at 20 °C was carried out by lowering the wax concentration stepwise (0.05% w/w) from a concentration roughly above the estimated CGC. The respective solution was cooled from 90 to 20 °C at a fixed cooling rate of 10 °C min^{-1}, a constant strain of 0.05%, and an angular frequency of 10 rad s^{-1}. Subsequently, samples were kept at 20 °C for 20 min, and a strain sweep was performed for each concentration step. The lowest concentration yielding $G' > G''$ was taken as the CGC for the respective wax/oil combination. It needs to be mentioned that samples might not be in a macroscopic solid state at this point, but the definition is in line with the rheological definition of a gel.[45]

Microscopy: Brightfield light microscopy (BFM) images were taken using the Axio Scope.A1 KMAT (Zeiss, Jena Germany) equipped with an AxioCam ICm1 Rev.1 camera. Samples were prepared similarly to those in Petri dishes. Hot solutions of 4% w/w wax in oil were pipetted on preheated microscope slides. After the cover glass was placed, samples were kept at 80 °C for 10 min. Then cooling rates of 10 and 0.05 °C min^{-1} were applied, analogous to the Petri dishes used for gel firmness. Images were taken after a storage time of 24 h at 20 °C without further processing (20× magnification).

In addition, preheated microscope slides were cooled from 80 to 10 °C at 10 °C min^{-1} using a temperature-controlled microscope unit (Linkam Scientific Instruments Ltd., Tadworth United Kingdom), and pictures were taken every 2.5 s. The image with the first visible crystals was taken as crystallization onset and compared to DSC onset.

All BFM-images were processed using ImageJ 1.52a software to derive quantitative information from BFM images. After scaling and thresholding, the number average crystal size [μm^2], the fractal dimension D, and the samples' 2-D porosity were calculated. The fractal dimensions were determined by using the box-counting method provided by ImageJ. All calculations were based on the evaluation of at least two images. For detailed information, please refer to ref. [46].

2.5. Statistical Analysis

All experiments were replicated according to the descriptions in the sections above. In tables, relevant findings were expressed as mean ± standard deviation. Statistical differences were determined using SPSS software, and running paired *T*-test or ANOVA and posthoc test (Bonferroni) analysis. The *p*-value was set to 0.05. In the results and discussion section, the oils stripped from minor components served as the reference. Posthoc tests were used to establish whether samples with minor oil components are significantly different from stripped samples. Moreover, it was assessed whether a further increase of PCs in heated oils affected oil and gel properties.

3. Results and Discussion

3.1. Oil Analysis

It has been recently reported that minor oil components have a considerable impact on the macroscopic and microscopic

European Journal of Lipid Science and Technology
www.ejlst.com

Table 2. Oil permittivity, free fatty acids, peroxide value, viscosity, water content, and polar components (from left to right) determined for stripped (P), natural (N), and various stages of deteriorated (0.5, 1.0, 2.5, 5.0, and 10.0) canola (C-) and sunflower (S-) oil. n.a. – not applicable.

Sample	ϵ [–]	FFA [mg/100 g]	PV [meq kg^{-1}]	η [mPa s]	H_2O [ppm]	PC ISO [g/100 g]
C-P	3.0027 ± 0.002	n.a.	0.1 ± 0.1	25.5 ± 0.02	13.4 ± 1.1	n.a.
C-N	3.0576 ± 0.002	4.0 ± 0.5	0.5 ± 0.1	33.2 ± 0.02	46.8 ± 4.4	3.8 ± 0.5
C-0.5	3.0678 ± 0.006[a)]	12.3 ± 31.9[a)]	5.4 ± 0.2[a)]	32.9 ± 0.10	192.7 ± 2.3[a)]	3.9 ± 0.4
C-1.0	3.0891 ± 0.006[a)]	3.8 ± 1.0	10.3 ± 0.4[a)]	32.6 ± 0.15[a)]	147.8 ± 1.6[a)]	4.9 ± 0.6[a)]
C-2.5	3.1078 ± 0.006[a)]	2.2 ± 0.4[a)]	17.9 ± 5.5[a)]	33.2 ± 0.20	197.1 ± 10.6[a)]	5.8 ± 0.7[a)]
C-5.0	3.1273 ± 0.006[a)]	2.3 ± 0.2[a)]	13.3 ± 1.2[a)]	34.4 ± 0.23[a)]	172.3 ± 1.4[a)]	8.6 ± 1.4[a)]
C-10.0	3.1673 ± 0.006[a)]	2.3 ± 0.5[a)]	17.1 ± 1.4[a)]	38.2 ± 0.10[a)]	267.1 ± 1.6[a)]	17.6 ± 1.4[a)]
S-P	3.0102 ± 0.003	n.a.	0.9 ± 0.3	21.4 ± 0.09	19.9 ± 1.2	n.a.
S-N	3.1225 ± 0.001	2.2 ± 3.1	2.6 ± 0.4	30.4 ± 0.05	224.0 ± 8.7[a)]	3.7 ± 0.2
S-0.5	3.1943 ± 0.006[a)]	2.8 ± 6.3	36.2 ± 1.1[a)]	30.2 ± 0.00	232.2 ± 19.8	4.7 ± 0.4[a)]
S-1.0	3.2143 ± 0.007[a)]	3.9 ± 1.4[a)]	43.5 ± 0.8[a)]	30.7 ± 0.34	195.7 ± 0.4[a)]	6.0 ± 0.2[a)]
S-2.5	3.2413 ± 0.006[a)]	1.9 ± 0.3[a)]	41.8 ± 3.5[a)]	31.9 ± 0.10[a)]	336.7 ± 28.2[a)]	8.7 ± 1.7[a)]
S-5.0	3.2683 ± 0.007[a)]	2.6 ± 1.3[a)]	63.3 ± 1.4[a)]	33.8 ± 0.00[a)]	529.6 ± 25.3[a)]	11.7 ± 1.8[a)]
S-10.0	3.3248 ± 0.007[a)]	4.8 ± 1.0[a)]	72.5 ± 0.1[a)]	38.0 ± 0.05[a)]	505.0 ± 4.8[a)]	19.4 ± 0.8[a)]

[a)] indicates significant difference between oils containing minor components. $p = 0.05$.

properties of sterol/sterol ester oleogels.[21,35] For studying their effect on wax oleogels, it appears necessary to determine basic oil quality parameters. **Table 2** shows the analytical data for stripped, untreated, and deteriorated canola (C-) and sunflower (S-) oil. It needs to be mentioned that natural and oils at all stages of deterioration—expressed as the increase in PCs—differ significantly from the stripped oils. Therefore, Table 2 only includes statistical significance ([a]) for oils containing minor components.

The purification treatments reduces the oils' permittivity, viscosity, water content, and eliminates FFAs and peroxides. Moreover, no polar components could be detected using the official method. On the other hand, most parameters presented in Table 2 increased significantly with each stage of oil deterioration. However, the increase was not continuous for FFAs, PV, and water content since these form and decompose during deterioration. Interestingly, the increase of oil permittivity from untreated oil (S-N) to the highest deterioration stage (S-10.0) was greater for sunflower oil ($\Delta\epsilon \approx 0.21$) than canola oil ($\Delta\epsilon \approx 0.11$). That is likely due to the formation of different reaction products indicated by the variations in PV, water content, and FFA development in both oils.

Additionally, sunflower oil contains more polar components at the end of the heating procedure, even though both oils contain similar amounts in their natural state. That is linked to the high polyunsaturated FAs (mainly linoleic acid) content in sunflower oil, which is generally more reactive than oleic acid, the main FA found in canola oil. However, samples with the highest oxidation level are only included in this study to highlight the changes introduced by nontriglyceride oil components and have no practical relevance.

One could argue that the increase in solvent viscosity impedes the formation of wax crystals during oleogel preparation by reducing the solutes' diffusion rate. However, temperature sweeps have shown that the viscosity difference around the relevant temperatures for gelation (50–60 °C) is almost negligible. In contrast, the firmness measurements were executed at ambient temperature. In that case, solvent viscosity might affect the results since it relates to the flow of the solvent through the crystalline network upon deformation.

3.2. Firmness

This section discusses the impact of oil type (degree of unsaturation, stripped oils) and content of PCs on wax oleogel firmness. The results are more descriptive at this point but will be put into context with, e.g., thermal behavior and microstructure later on.

Effect of Oil Type: The firmness of oleogels utilizing stripped canola or sunflower oil and cooling rates of 10 and 0.05 °C min^{-1} are depicted in **Figure 2**. The columns without a pattern (black: canola; white: sunflower) are related to the high cooling rate, while columns with a pattern represent the firmness of samples prepared at 0.05 °C min^{-1} (dotted: canola; striped: sunflower). In line with the literature, SFX oleogels are the hardest, irrespective of oil type and cooling rate, while BWX samples are the softest.[1,47]

There is no significant difference connected to the type of oil in SFX, BWX, and CLX. However, in RBX samples, more unsaturated oil produces harder gels.

In contrast, the cooling rate significantly changes the oleogel firmness of SFX and RBX gels, while there was no considerable difference in BWX and CLX samples.

Surprisingly, cooling at 0.05 °C min^{-1} resulted in significantly softer gels for SFX, while RBX-based gels became harder at the low cooling rate. In general, a lower cooling rate enables highly ordered crystals which are usually larger (lower supersaturation) due to a shift in the balance of nucleation and growth rates. Consequently, the formation of separate instead of mixed crystals is likely. In line with that, RBX samples cooled at 0.05 °C min^{-1} show high deviations in gel firmness compared to the gels produced with 10 °C min^{-1}. That indicates the formation

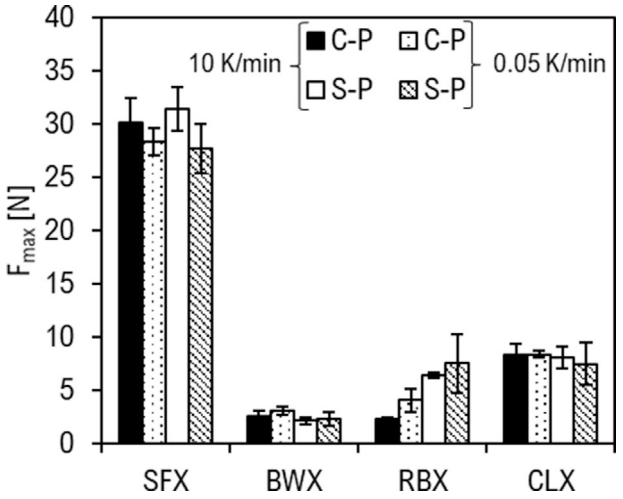

Figure 2. Firmness of oleogels prepared using purified sunflower or canola oil and 10% w/w sunflower (SFX), bees- (BWX), rice bran (RBX), or candelilla wax (CLX), cooled at 10 (black and white columns) or 0.05 °C min^{-1} (pattern-filled columns).

of inhomogeneous areas within the Petri dish potentially caused by separate crystallization. On the other hand, in BWX and CLX samples, oleogel hardness seems to be independent of the cooling rate and the type of oil used.

Effect of PCs: The hardness data depicted in Figure 2 was further used as the reference to relate the data of oleogels from untreated and deteriorated oils. These gels were subjected to the same cooling rates. **Figure 3** depicts the relative oleogel firmness of canola (A, B) and sunflower oil (C, D) oleogels over PC content (Table 2). The first group of columns relates to gels made with untreated canola oil (PC 3.8 and 3.7). Column groups 2, 3, 4, 5, and 6 relate to the oil deterioration stages (see Table 2). It should be mentioned that the statistical correlation of gel hardness and several oil quality parameters such as PV, FFA and water content was, to the greatest possible extent, inconclusive.

However, distinct trends can be seen for the type of wax, the cooling rate, and the oil used. For example, at 0.05 °C min^{-1} the hardness of SFX gels is significantly higher at the lowest two PC levels (Figure 3A,C). In contrast, there is no significant difference to the reference at higher PC content. For the high cooling rate, changes in gel hardness are insignificant. Hence, it is fair to assume that SFX's network is not primarily affected by the type and concentration of PC but the cooling rate.

In contrast, RBX oleogels are significantly firmer with increased PC levels in canola oil, and the effect is more pronounced for samples cooled at 0.05 °C min^{-1}. Similar to the results reported for hardness in stripped oils, the deviations are relatively high in gels subjected to 0.05 °C min^{-1}. In general, BWX and RBX samples are the softest. Therefore, slight changes in gel firmness result in significant differences in relative hardness. Hence, the trends seen in Figure 3 could be disproportionate. Interestingly, for sunflower oil (Figure 3C,D), RBX gel hardness appears not significantly different from the reference at 0.05 °C min^{-1}. However, at 10 °C min^{-1}, a significant reduction in gel hardness occurred on PC increase. Still, it is essential to note that the initial hardness values of RBX in stripped sunflower oil were considerably higher than in canola oil (Figure 2). However, that does not fully explain the significant drop (up to 60%) in gel hardness at high cooling rates. Thus, the RBX crystal network's firmness seems to be affected by the type of oil and its deterioration products.

The hardness of BWX oleogels appears to be more sensitive to the cooling rate. All samples containing PCs were significantly softer than the reference at lower cooling rates (Figure 3A,C) without a clear relation to the PC level. However, the opposite trend on increasing PC levels was observed at high cooling rates, whereas the effect is much more pronounced in sunflower oil (Figure 3B,D). Like RBX, the firmness of all gels was very low. Again, the trends seen in Figure 3 could be disproportionate.

At 0.05 °C min^{-1}, BWX in sunflower oil decreases gel hardness' for all TPC levels. That is in line with the observation in gelled canola oil. However, the gels become significantly firmer with increasing PC content at 10 °C min^{-1}. That was observed in canola oil to a much lesser extent. Since BWX contains components different from WE (Table 2), this effect likely relates to the synergistic effects of oil deterioration products. However, BWX oleogel hardness appears to be sensitive to both cooling rate and the content of polar components, while the type of oil is negligible.

Finally, CLX oleogels showed lower gel hardness than the reference in both oils when cooled at 0.05 °C min^{-1}, whereat the difference was not always significant. However, in oils with high PC content (Figure 3A at 17.6 and Figure 3C at 11.7 and 19.4), a significant increase in gel hardness was observed, indicating either a modification of CLX solubility or a substantially different crystal structure or network interactions. When using the high cooling rate, CLX firmness appeared independent of the PC level (except canola oil 17.6). That indicates that CLX network firmness is affected by the cooling rate and PC content and only marginally by the type of oil used.

In summary, PCs seem to have distinct effects on the oleogels for the wax types studied, while the unsaturation of the oil does not seem to have a significant impact. At this point, it remains unclear whether these observations are related to changes in wax solubility, crystal morphology, network interactions, or a combination of those. Consequently, the thermal behavior of the gels was studied to address the first parameter.

3.3. Thermal Behavior

Since the effect of PC increment on oleogel firmness is most pronounced for the highest content of PC except a few exceptions, in the following, only the results obtained using stripped (–P), untreated (–N), and most deteriorated oil with the highest PC content (–D) will be compared.

DSC measurements were performed to validate whether the effects on oleogel hardness are related to wax solubility modifications. Moreover, studying the thermograms allows identifying distinct crystallization or melting events induced in the presence or absence of PC.

Figure 4 shows the transition enthalpies during gel dissolution (endothermic > 0) and gel formation (exothermic < 0), plotted on the left vertical axis. The right vertical axis displays the respective transition temperatures of wax oleogels from stripped canola

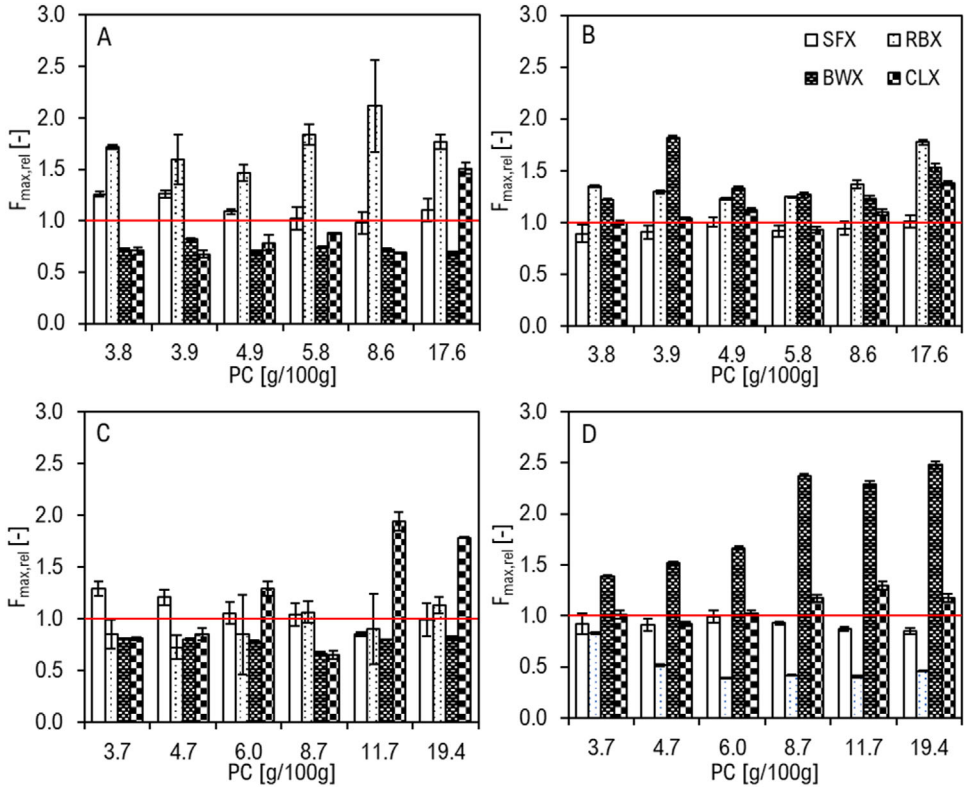

Figure 3. Relative hardness of 10% w/w A,B) canola and C,D) sunflower oil oleogels over PC content determined using the official method. A,C: Slow cooling (0.05 K min^{-1}), B,D: Fast cooling (10 K min^{-1}). Red line indicates the reference value.

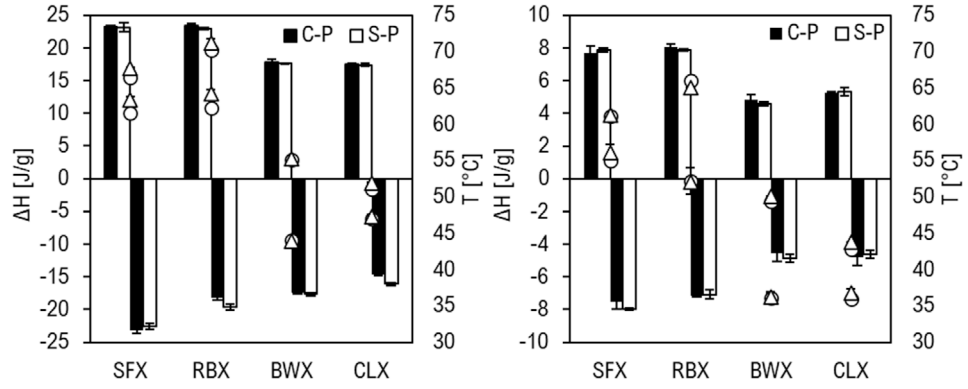

Figure 4. Enthalpy (endothermic > 0, exothermic < 0) of gel dissolution and gel formation (columns, left vertical axis) and dissolution and gelation temperatures (symbols, right vertical axis) of wax oleogels of purified canola (C-P, circles) and sunflower oil (S-P, triangles). Left figure: 10% w/w wax; right figure: 4% w/w wax. Samples were cooled and heated at 10 K min^{-1}.

(circles) and sunflower oil (triangles). The higher temperature always relates to gel dissolution's peak temperature and the lower temperature to the peak during gel formation. The left figure depicts the data of 10% w/w oleogels, while 4% w/w wax were used on the right. Samples with 4% w/w wax were produced to intensify the impact of polar components introduced when untreated and deteriorated oils were used (discussed further down).

The results in Figure 4 serve two purposes. On the one hand, it validates the applied method and serves as a reference for oil quality effects. Indeed, comparing the left and right graphic of Figure 4, one can assume that the behavior of a specific wax type is independent of the wax concentration and oil type. There were no significant differences in the transition enthalpies between oleogels comprising either stripped canola or sunflower oil.

Overall, SFX and RBX samples showed the highest transition enthalpies. That is due to their high WE content (see **Table 3**). The minute enthalpy difference between dissolution and formation—formation in line with expectation slightly lower—suggests that neither additional crystallization nor polymorphic transitions occurred during stabilization (20 min). Preliminary stabilization

Table 3. Chemical composition of waxes in % adapted.[22]

	SFX	RBX	BWX	CLX
HC	0.2	0.3	26.8	72.9
WE	96.2	93.5	58.0	15.8
FFA	3.3	6.0	8.8	9.4
FA-OH	0.3	0.2	6.4	2.2

tests over 72 h at 20 °C showed no postcrystallization events in oleogel samples (data not shown). In line with the higher WE chain length, the dissolution temperature of RBX is higher than SFX.

Interestingly, the gap between gel formation and dissolution is more significant in RBX samples, implying that the WEs composition of SFX enables better nucleation (Figure 4). That is likely related to the smaller chain length span within the WE-fraction of SFX compared to RBX.[22] Indeed, network formation was found to be promoted in WE compositions with narrow chain length distribution.[23] However, there seems to be a small effect of the oil type on the solubility of SFX and RBX since the dissolution, and the gel formation temperatures are slightly higher in stripped sunflower oil. However, this observation could not be reconfirmed in 4% w/w oleogels and is possibly related to minor deviations caused during sample preparation.

In BWX and CLX gels, gel formation and dissolution temperatures appear independent of the oil type. For BWX-based oleogels, a larger undercooling than in CLX-based gels was observed, which could be caused by the differences in the composition's heterogeneity (Table 3). CLX is characterized by a dominant component comprising about 60% w/w of C31 HC.[22] Unlike the other waxes studied, there is a considerable discrepancy between the transition enthalpies in CLX, indicating the crystallization process of the secondary components (19% WE and 9% FFA) was not completed during the cooling and stabilization process. However, the data in Figure 4 establish a sound base as a reference point for the quantification to evaluate changes introduced by the presence of minor polar components.

Figure 5 shows the relative dissolution enthalpies of 4% w/w oleogels utilizing untreated (–N) and deteriorated (–D) canola (left) and sunflower oil (right). Again the data has been related to that of oleogels from stripped oils. For all samples, the enthalpy is significantly lower than the reference. However, the magnitude appears somewhat different for canola and sunflower oil.

For SFX samples, varying the oil type and level of PCs (untreated vs deteriorated) does not have a considerable effect. That is in line with the results on gel hardness (Figure 3). In contrast, the drop in dissolution enthalpy is more significant in RBX samples (up to 38%) and seems to vary with the PC content and oil type (larger effect in canola oil). Remarkably, this evolution of values does not seem to correlate to the gel hardness (Figure 3).

Similarly, the increase in BWX oleogel hardness does not correlate with the data obtained for dissolution enthalpies. Moreover, there is no clear correlation with the oil type. In both oils, the enthalpies are reduced, but the effect is again more pronounced in canola oil samples.

In CLX oleogels, the dissolution enthalpy is reduced by about 10% in untreated oil and about 16% in high-PC oils. Here, both oils show comparable results, and an increase in dissolution enthalpy with a higher PC content can be observed, in line with the results on gel hardness.

Overall, the dissolution enthalpy results remain inconclusive and cannot be put into context with other parameters. Nevertheless, the enthalpy is significantly reduced in all samples containing PCs, relating to the assumption that the build-up of highly ordered crystalline structures is less disturbed in stripped oils than in systems containing PCs. However, these differences do not automatically increase oleogel hardness since other factors such as crystal network interactions, crystal size, and surface. A lower dissolution enthalpy in oils containing polar components suggests a modified solubility of the waxes, which might arise from solute-solute (PC-wax) interactions. However, that implies that more material remains dissolved after equilibrium has been reached, resulting in lower dissolution temperatures. Interestingly, the oleogel dissolution and formation temperatures were practically invariant for all waxes and independent of the oil type (**Figure 6**A,B).

Figure 6 (top) shows that the dissolution temperature does not vary significantly with the PC content for oleogels produced at 10 °C min^{-1}. Hence, there is no considerable effect on wax solubility within the range studied. However, the peak formation temperature appears to be slightly modified in the presence of PC, shown in Figure 6C,D.

Although the formation is subjected to somewhat greater deviations, distinct effects can be seen for the different wax types. The formation of SFX oleogels is not considerably affected by PCs. In contrast, there is a slight decrease in gel formation temperature for RBX, BWX, and CLX samples. However, this appears

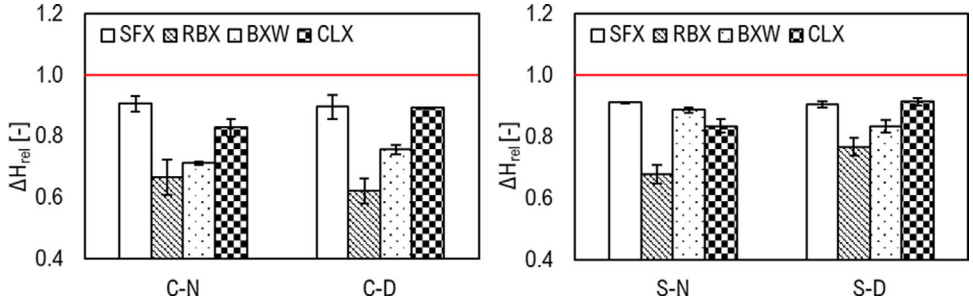

Figure 5. Relative dissolution enthalpy of wax oleogels (4 % w/w). Left: canola and right: sunflower oil. –N indicates untreated oils and –D oils with the highest PC content. Samples were cooled and heated at 10 K min^{-1}.

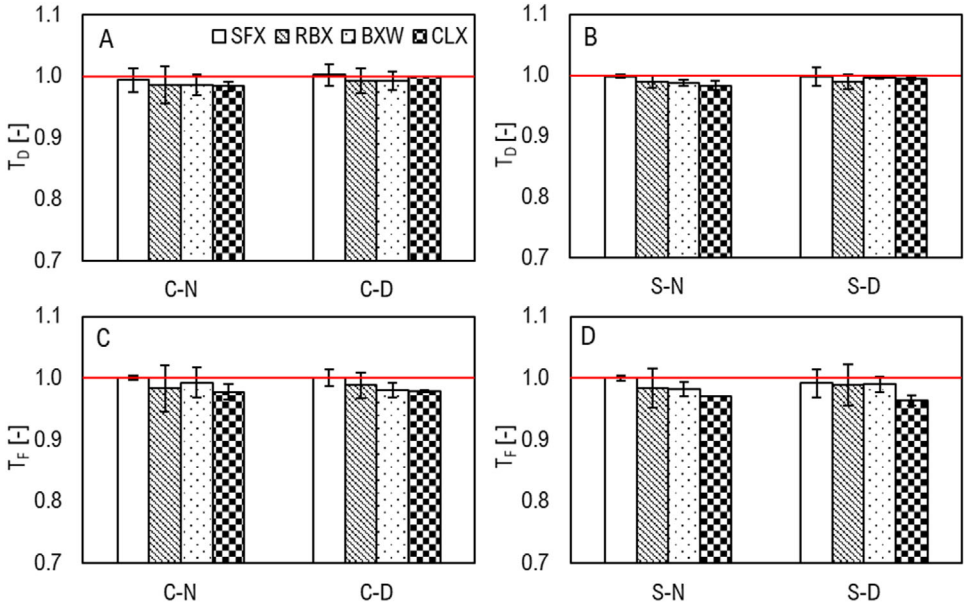

Figure 6. A,B) Relative gel–sol temperature and C,D) relative sol–gel temperature of wax olgeogels. A,C: canola oil; B,D: sunflower oil. All gels prepared with 4 % w/w wax. –N indicates untreated oils and –D oils with the highest PC content. Samples were cooled and heated at 10 °C min^{-1}.

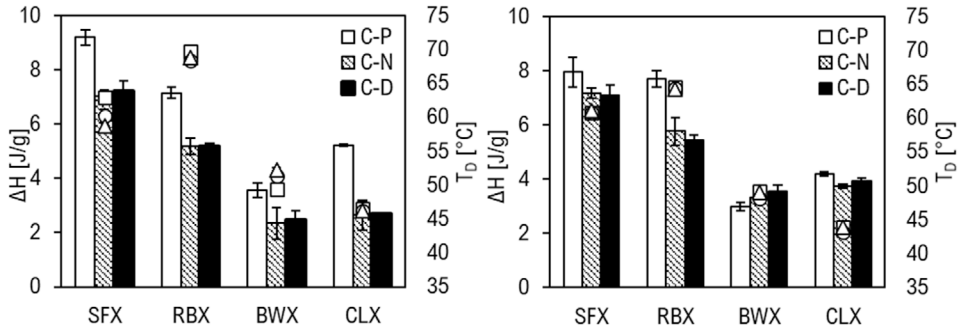

Figure 7. Dissolution enthalpy (columns, left vertical axis) and dissolution peak temperature (symbols, right vertical axis) of 4% w/w wax oleogels from purified (C-P, squares), untreated (C-N, circles) and deteriorated (C-D, triangles) canola oil. Left graphic: gelation at 1 °C min^{-1}, right: gelation at 40 °C min^{-1}.

to be independent of the oil type and could result from weak interactions, retarding the formation of wax crystals. Substantial effects on the gel formation temperature, similar to those reported for the sterol/sterol ester systems, cannot be seen.[35] The self-assembly and structuring of the sterol/sterol ester structuring system widely depend on hydrogen bonds. Hence, they are prone to the presence of polar components able to form similar bonds.[48,49]

In contrast, the formation of wax crystals is much less dependent on hydrogen bonds. Only FFA and FAL may form hydrogen bonds with polar molecules through carboxyl or hydroxyl groups. However, their content varies in the waxes studied (3.5% SFX, 6.2% RBX, 15.1% BWX, and 11.6% CLX[22]), and their arrangement in the nonpolar triglyceride oil is unknown. Potentially, in a dissolved state, they form clusters with the polar head groups facing each other.

However, the data on oleogels firmness (Figure 3) suggests that different structures might form depending on the cooling rate. To this end, samples of stripped, untreated, and deteriorated (highest PC) canola were subjected to a fast (40 °C min^{-1}) and slow (1 °C min^{-1}) gelling procedure, followed by an isothermal period of 20 min at 10 °C. Subsequently, the gel dissolution was recorded at 10 °C min^{-1}.

Figure 7 shows the dissolution enthalpies (columns) and gel-sol transition peak temperatures (symbols) of these oleogels. The dissolution temperatures are not significantly different in samples containing PCs in fast-gelled samples (Figure 7 left). Even though the dissolution temperatures vary a bit more with PC at 0.05 °C min^{-1}, the differences are insignificant. Hence, the low cooling rate likely induces this variation (Figure 7, right). The fact that the slowly crystallized sample always shows higher gel–sol transition temperatures confirms the above statement. It is also confirmed that this kinetic depression effect is least pronounced in more homogenous waxes, SFX and CLX. That is in line with the observation that the enthalpy of dissolution is lower for fast cooled samples based on stripped oils.

These might show a suboptimal crystal packing due to kinetic effects or be based on energetically less favorable kinetically induced mixed crystals. Considering the effect of PC on the enthalpy of transition, it is fair to conclude that no difference between the two PC levels could be identified throughout all samples. The reduction encountered on PC presence is more pronounced in samples after cooled ad 0.05 than at 10 °C min^{-1}. However, this statement is misleading because, in the presence of polar components, the enthalpy of dissolution in SFX and RBX appears to be independent of the cooling rate. In samples based on CLX and BWX, the enthalpy of gel–sol transition is higher for PC-containing samples when the cooling rate is high. A possible explanation of this finding based on the contribution of crystallized FFA's, which are present in both waxes and deteriorated oils, falls short because of the strong dependency of the observation on cooling rate.

3.4. Rheology – CGC

Regarding oleogels, the solvent composition (PC and TAG composition) could also affect some commonly measured parameters such as gel hardness and critical gelling concentration (CGC). The latter is usually postulated as the minimum concentration of a gelator to produce a non-flowing state. However, it is often determined arbitrarily by increasing the wax concentration gradually, using large increments and different procedures. Hence, the relevant literature reports very diverse values of CGC for the same type of wax (Table 1). Table 1 shows the CGC found in the literature of SFX, RBX, CLX, and RBX, the concentration increase used (Δ% w/w), the oil type, and the determination method. Considerable variations of CGC can be seen for all wax types. These are related to the individual wax constituents, the increment of concentration, and the oil type. It is crucial to consider the impact of oil composition since the FA profile of triglycerides (TAGs) might affect wax solubility (solvent-solute interactions). Besides, dissolved minor polar oil components could interfere with the self-assembly of the structurants by forming similar interactions to those between wax components explained earlier (solute–solute interactions). Only one publication considers a combined approach, where a range of concentrations was prepared, and samples were flipped over to determine the non-flowing state at 5 °C (Table 1).

Subsequently, dynamic-mechanical-thermal analysis (DMTA) (temperature sweep at low oscillation and frequency) and amplitude sweeps were used to detect the lowest concentration at which $G' > G''$. Unfortunately, the increments are large (0.5% w/w), and it remains undisclosed if the samples used for the flow test were transferred onto the rheometer or if hot wax solutions were used for DTMA. Transferring viscous samples partly breaks up structures and generates falsified results.

However, the results render the flow-test determination of CGC very unprecise, subjective, and unsuitable for scientific publications since the CGC is regularly used to characterize the oleogel system further. Besides, if a sample's flowing is solely considered, the CGC also appears unpractical for product applications since it provides no useful information about consistency and sensitivity.

A precise method to determine CGC was developed within this study to study the differences introduced by PCs. **Figure 8** (right) shows the data for all wax oleogels as a function of solvent permittivity for either stripped (lowest ϵ), untreated (moderate ϵ), or deteriorated (highest ϵ) canola (filled symbols) or sunflower oil (open symbols). In line with the flow test results reported in the literature (Table 1), the rheological CGC increases in the order SFX < CLX < RBX < BWX. Again this underlines that the generation of a solid-like structure in wax oleogels is promoted by (1) high WEs content and (2) a limited difference in WE chain length (SFX), and (3) more homogenous composition with high concentrations of components that co-crystallized (HC, predominantly C31 in CLX).

For all waxes studied, the data gathered here indicate a lower CGC than given in Table 1. In general, the presence of PCs significantly reduces the CGC of all waxes but SFX. This effect is more pronounced in BWX. None of the systems appeared to be sensitive to the variation in the level of PC. Nevertheless, in stripped oils, the CGC appears independent of the oil type (Figure 8). Simultaneously, there are minor variations between canola and sunflower oils containing PCs, likely caused by the differences of the non-TAG molecular species.

However, the reduction of CGC with PCs leaves two possible explanations: the polar components could contribute to establishing a space-filling scaffolding so that gelation can be achieved at lower levels of solid material. That is in analogy to the contribution of small amounts of emulsifiers to fat crystal networks.[14,17] Alternatively, PCs might reduce the solubility of the waxes in the oil. Therefore, the necessary amount of solid material to form a gel is lower. However, the second interpretation is in conflict with the increase in gel–sol transition enthalpy in gel from stripped oils reported in the previous section.

Moreover, gel dissolution temperatures were invariant, indicating no substantial changes in wax solubility. Consequently, a synergistic effect of PCs on network formation appears likely.

At this point, it has to be discussed what is necessary to create a structure where $G'' > G''$. Initially, there has to be supersaturation which leads to nucleation and growth of wax crystals. Therefore, another approach to process the DSC data is presented in **Table 4**. The gel–sol transition enthalpy data for two wax concentrations (4%, 12% w/w) allows estimating the enthalpy of melting of 100% wax ($\Delta H_{pure,calc}$). Dividing the difference in the two samples gel–sol enthalpies by their concentration yields the melting enthalpy when dissolution effects and the temperature at which the transition from solid to liquid occurs are ignored. The data for gels with stripped oils are in good agreement with pure waxes' actual values (ΔH_{pure}). The values obtained gels from untreated and deteriorated oils are, except RBX gels, lower. These reduced values of the normalized slid to liquid transition enthalpy indicate that PCs support dissolution. That is in line with the fact that the lowest solubility was recorded for stripped oils. Furthermore, the data enable determining the amount of dissolved material in stripped oils (x_{diss}% w/w) by plotting the dissolution enthalpy over structurant concentration and extrapolating $\Delta H = 0$. The values of x_{diss} have per definition to be lower than the CGC. For the stripped oil oleogels, this condition is satisfied and allows determining the amount of solid material present at CGC (Table 4). The values generated are very low, 0.075–0.722% w/w. However,

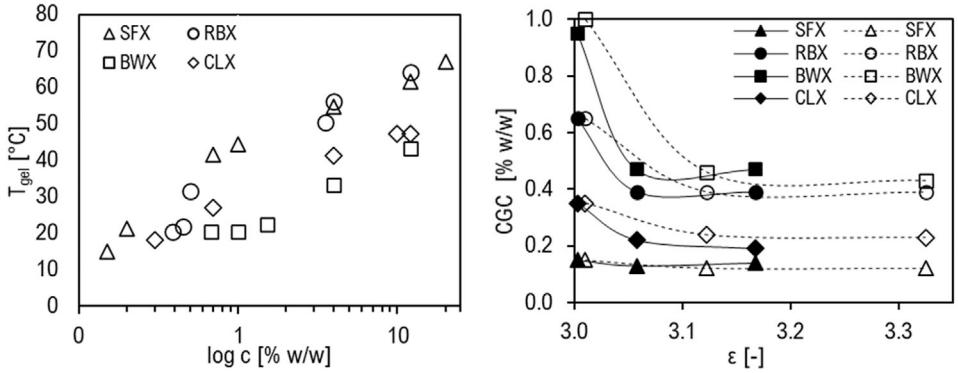

Figure 8. Left: CGC measurements for various wax concentrations (c [% w/w]) in natural canola oil to estimate the CGC at 20 °C, *x*-axis logarithmic scale. Right: CGC of waxes in purified (lowest ϵ), natural and deteriorated (highest ϵ) oil, filled symbols: canola oil; open symbols: sunflower oil.

Table 4. Validation of CGC determination, x_{diss} -amount of wax dissolved in stripped oil, CGC%- CGC in stripped oil, ΔH_{pure} -dissolution enthalpy pure wax, $\Delta H_{pure,calc}$ dissolution enthalpy pure wax extrapolated from ΔH of 4% and 12% w/w wax oleogels.

	x_{diss} % w/w	CGC % w/w	CGC-x_{diss} [% w/w]	ΔH_{pure} [J g^{-1}]	C-P $\Delta H_{pure,calc}$ [J g^{-1}]	C-N $\Delta H_{pure,calc}$ [J g^{-1}]	C-D $\Delta H_{pure,calc}$ [J g^{-1}]
SFX	0.075	0.15	0.075	195	194	173	167
RBX	0.153	0.65	0.497	187	191	194	197
BWX	0.228	0.95	0.722	160	161	159	147
CLX	0.228	0.35	0.122	146	151	139	139

the values of x_{diss} have to be lower than the CGC, which is valid for all waxes using stripped oil. In oils comprising PC, the calculated dissolution enthalpy did not agree with that of pure wax. Hence, the calculated dissolved material is always higher than the CGC, independent of whether the actual dissolution enthalpy of pure wax or the calculated values were chosen. That results from the overall lower dissolution enthalpy in oils comprising PC (see section DSC). However, if the calculated ΔH overshoots the actual value, interactions between the network particles can be assumed and vice versa. Hence, in oils with PC, only RBX shows increased crystalline interactions in the presence of PCs. That conflicts with the lower CGC in these oils, indicating that the establishment of inter-crystalline bonds might be promoted with PC. However, the number of these interaction points highly depends on the number of crystals and their surface area (size-related).

3.5. Rheology – Strain Sweep

Strain sweeps of 10% w/w oleogels were used to determine the maximum G' within the LVR as well as the $\Delta G''$ and γ_{max} (see Figure 1 for details).

Figure 9 shows the results of the relative values of G''_{max}, $\Delta G''$ and γ_{max}. The values were always related to those of the respective stripped oil. Unfortunately, at 10% w/w wax concentration, the results of G''_{max} are less expressive due to the high wax concentration. That leads to relatively large deviations between the repetitions since the networks are very dense.[3,23] Repeating the experiments at, e.g., 4% w/w wax concentration would hence be beneficial. However, the break-up behavior shows a much better response at high wax concentrations.

Nevertheless, Figure 9A illustrates the relative G''_{max} values for all waxes in untreated and deteriorated oils (reference is stripped oil). Various studies reported the absolute values of G'' for different waxes, which increase in the following order RBX < CLX < BWX < SFX.[22,23,50] In SFX samples, there is no considerable effect considering the type of oil and PC concentration. However, the results indicate a higher G''_{max} for gels from oils containing PCs, which relates to more interaction points within the network.[45] Considering the firmness of SFX oleogels, this does not necessarily translate into a higher penetration hardness (Figure 3). The G''_{max} of RBX oleogels seems to be largely independent of PCs but is also subjected to irregularities, especially at the highest PC concentration for both oils. In contrast, in BWX and CLX samples, there appears to be an increase of G''_{max} when utilizing oils with the highest PC. However, when utilizing untreated oils, CLX samples show a lower G''_{max} than the reference, while in BWX gels, it is slightly higher.

It remains unresolved whether the increase observed in some samples results from the formation of additional connection points in the network due to PCs or smaller crystals, which provide a larger structuring surface. Vice versa, a decrease could be linked to the formation of larger crystals or the prevention of crystal–crystal interactions due to high amounts of PCs blocking the interaction points, similar to the results reported for fat crystal networks.[17]

Figure 9B shows $\Delta G''$ determined for gels based on PC-containing oils according to Figure 1. Again, all values are considerably higher than in the reference. Moreover, the effect is most extensive in RBX oleogels and lowest in SFX's highly ordered structure. In SFX, BWX, and CLX samples, a further

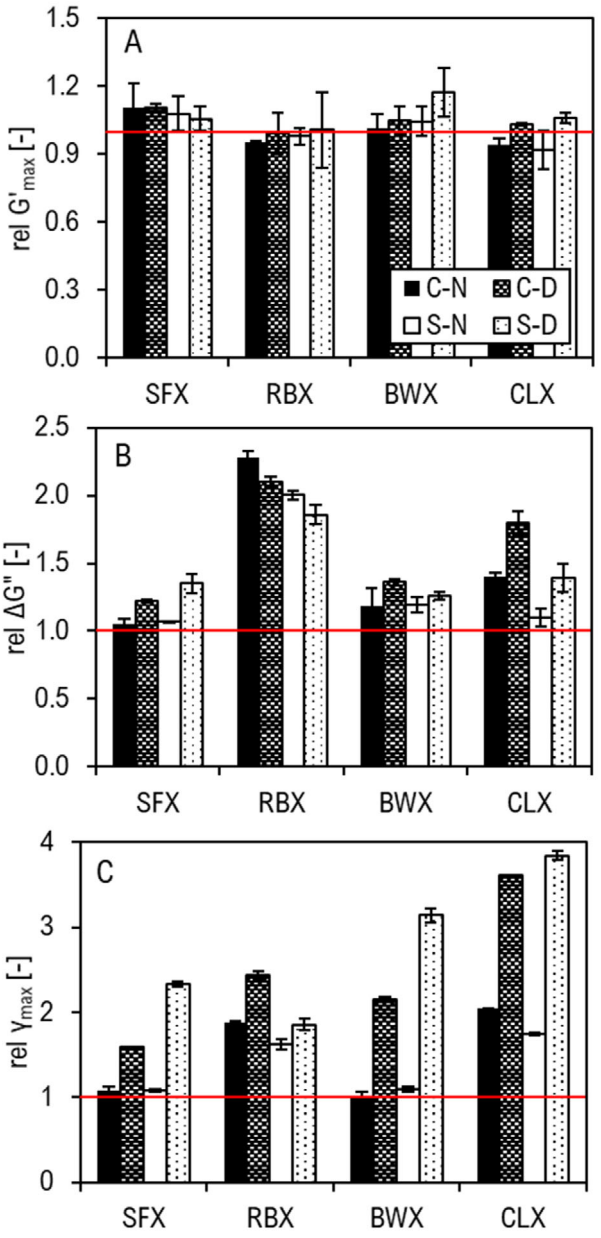

Figure 9. Relative values of A) G'_{max} within the LVR, B) $\Delta G''$ during amplitude sweep and C) γ_{max} representing the end of the LVR. Samples gelled under low oscillation conditions at 10 K min^{-1}. All samples with 10% w/w wax. C-X canola oil; S-X: sunflower oil. X: N-untreated, D-deteriorated (highest PC).

increase of $\Delta G''$ can be seen comparing oils utilizing untreated and deteriorated oil. Generally, G'''' describes the portion of deformation energy lost by internal friction. As the strain increases during amplitude sweeps (before the flow point), individual network bonds rupture. The break-up relates to their individual strength. However, these movable network fragments show internal friction increasing G'' until the sample starts to flow. Hence, network interactions appear to be modified in gels with PCs so that more fragments form during the sweep, causing higher internal friction. A similar effect has been reported in the presence of PCs for sterol/sterol ester oleogels.[21,36]

Finally, Figure 9C depicts the strain at which the sample starts to be irreversibly damaged, which relates to the systems' ability to store deformation energy during amplitude sweeps. The value was determined in agreement with the official methods defining the end of the LVR as the strain at which G' deviates by 5% from its maximum value.[44] In SFX and BWX oleogels, there is no apparent difference to the reference when untreated oils are used. In contrast, in RBX and CLX samples, γ_{max} is considerably higher than in the reference sample. Clearly, γ_{max} increases tremendously in oleogels utilizing oils with the highest PC levels, and the effect is highest in BWX and CLX samples. That might relate to the crystalline network formed in these samples, whereas smaller network structures are known to store deformation energy better.[45]

In summary, wax oleogels appear to store deformation energy better if PCs are present in the continuous phase, and the effect depends on the PC level. However, there is also more internal friction due to loose aggregates once the sample is irreversibly damaged but macroscopically intact. That shows that the network interactions are significantly modified in the presence of PC, but that does not necessarily translate into equal changes in macroscopic properties such as hardness. Nevertheless, these modifications are likely linked to the specific network features present in each wax's oleogel. Their appearance and potential alterations in the presence of PC will be discussed in the following.

3.6. Microscopy

The crystal size and number, their interactions (e.g., sintering), and the general arrangement of the crystal network are vital for the macroscopic properties of wax oleogels, such as hardness.[54] Therefore, this section presents and discusses the microstructure of 4% w/w wax oleogels cooled at 10 and 0.05 °C min^{-1} in the context of the results presented in the previous sections.

After gelation, tile images were taken of all samples to identify representative areas. Subsequently, two images of the typical structures were captured and processed using ImageJ software. The box-counting fractal dimension (D), average crystal size [μm^2], and the porosity of each sample are shown in **Table 5**. The latter is a measure of the magnitude of crystal-free space in the sample. In contrast, the fractal dimension relates to the spatial distribution of the crystals, indicating the homogeneity of their distribution. Hence, higher D-values connect to more evenly filled samples. In general, it is expected that at lower cooling rates, larger crystals form due to lower supersaturations. Thus, the porosity likely increases while the fractal dimension decreases. The image analysis was performed similarly to previous studies, and the magnitude of values obtained is in good agreement with the literature for a similar sample preparation procedure.[55] Although the crystal size results were often inconclusive due to either very small crystals indistinguishable from one another or poor contrast between crystal and background, they were still included for completeness.

Figures 10–13 show brightfield images of SFX, RBX, BWX, and CLX, respectively. The top 3 images (A–C) show samples

Table 5. Results of image analysis using Image J software for 4% w/w canola oil wax oleogels.

	Oil	Cooling rate [°C min^{-1}]	Ø size [μm^2]	Fractal dimension *D* [–]	Porosity [–]
SFX	C-P		5.58±1.53	1.85±0.03	0.73±0.035
	C-N	10	9.38±0.51[a)]	1.90±0.01[a)]	0.71±0.011
	C-D		4.92±0.12[a)]	1.77±0.00[a)]	0.78±0.002[a)]
	C-P		2.29±0.22	1.59±0.06	0.90±0.032
	C-N	0.05	4.58±0.19[a)]	1.74±0.06[a)]	0.80±0.010[a)]
	C-D		3.38±0.20[a)]	1.58±0.06	0.88±0.023
RBX	C-P		5.48 ±1.06	1.62±0.03	0.84±0.044
	C-N	10	10.02±0.90[a)]	1.56±0.05[a)]	0.88±0.040[a)]
	C-D		6.96±0.59[a)]	1.50±0.01[a)]	0.90±0.017[a)]
	C-P		3.55±1.28	1.58±0.26	0.82±0.007
	C-N	0.05	2.41±0.19[a)]	1.43±0.04[a)]	0.93±0.020[a)]
	C-D		3.55±0.46	1.54±0.01	0.87±0.035[a)]
BWX	C-P		8.59±1.43	1.92±0.01	0.63±0.021
	C-N	10	4.24±0.04[a)]	1.84±0.03[a)]	0.73±0.004[a)]
	C-D		6.31±1.30[a)]	1.88±0.02[a)]	0.68±0.019[a)]
	C-P		3.91±0.22	1.83±0.01	0.67±0.023
	C-N	0.05	5.15±0.72[a)]	1.92±0.00[a)]	0.74±0.006[a)]
	C-D		9.58±0.09[a)]	1.84±0.01	0.85±0.019[a)]
CLX	C-P		4.45±2.82	1.90±0.03	0.74±0.007
	C-N	10	4.79±1.99	1.91±0.02	0.73±0.101
	C-D		3.65±1.93	1.91±0.03	0.70±0.045
	C-P		8.10±0.23	1.94±0.05	0.63±0.002
	C-N	0.05	7.67±0.09	1.83±0.01[a)]	0.74±0.031[a)]
	C-D		7.67±0.26	1.88±0.03[a)]	0.71±0.026[a)]

[a)] indicates significant difference to stripped oil. $p = 0$.

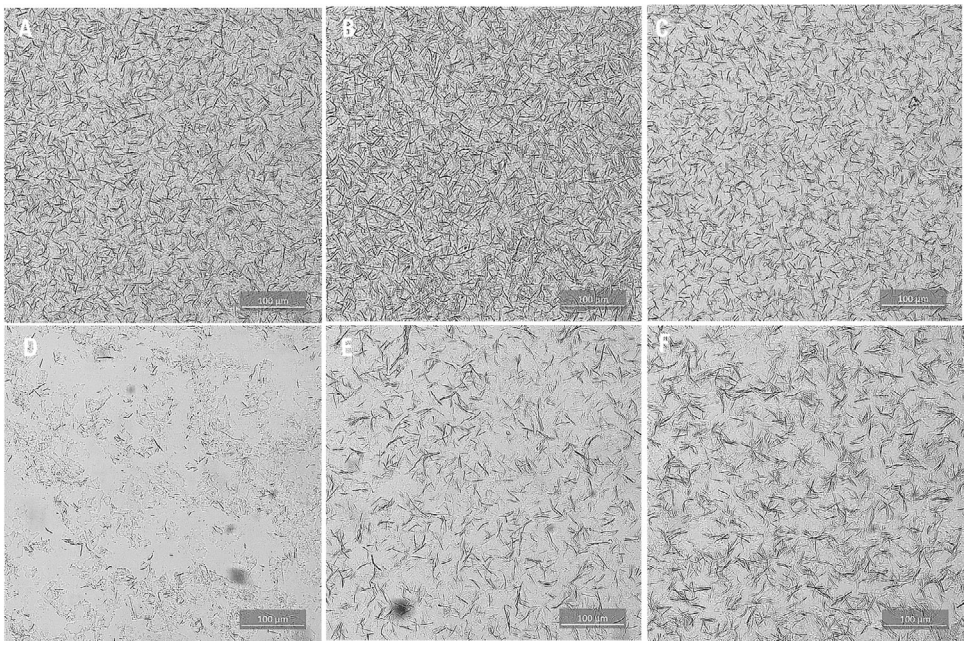

Figure 10. Images of 4 % w/w SFX oleogels. A–C) cooled at 10 K min^{-1}, from left to right: stripped (A), untreated (B), and deteriorated (C), highest PC) canola oil. Bottom: cooled at 0.05 K min^{-1} from left to right: D) stripped, E) untreated, and F) deteriorated, highest PC) canola oil. Scale bar: 100 μm.

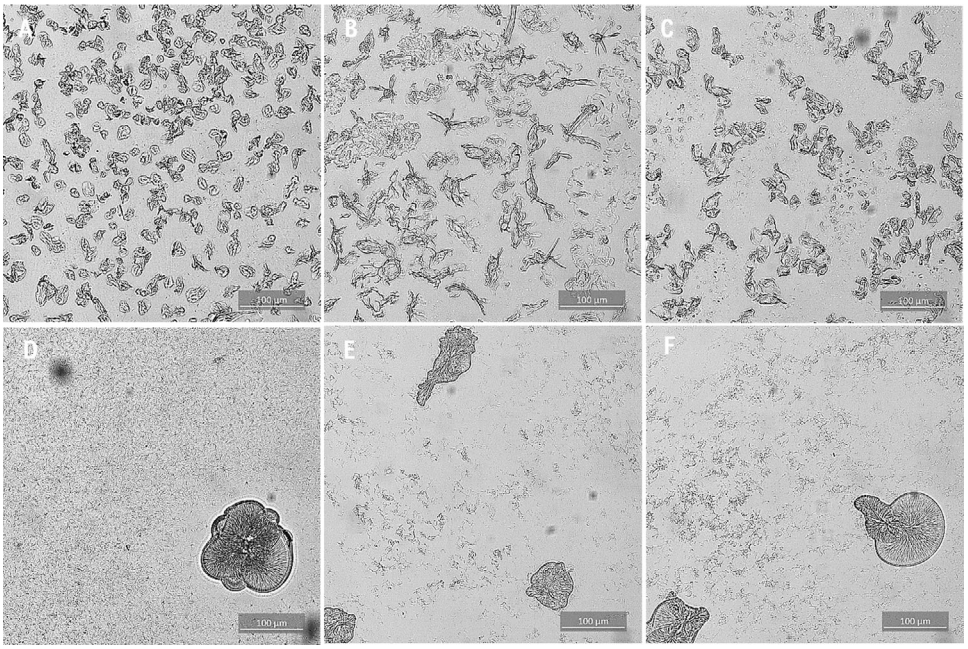

Figure 11. Images of 4% w/w RBX oleogels. A–C) Cooled at 10 K min^{-1}, from left to right: stripped (A), untreated (B), and deteriorated (C), highest PC) canola oil. Bottom: cooled at 0.05 K min^{-1} from left to right: D) stripped, E) untreated, and F) deteriorated, highest PC) canola oil. Scale bar: 100 µm.

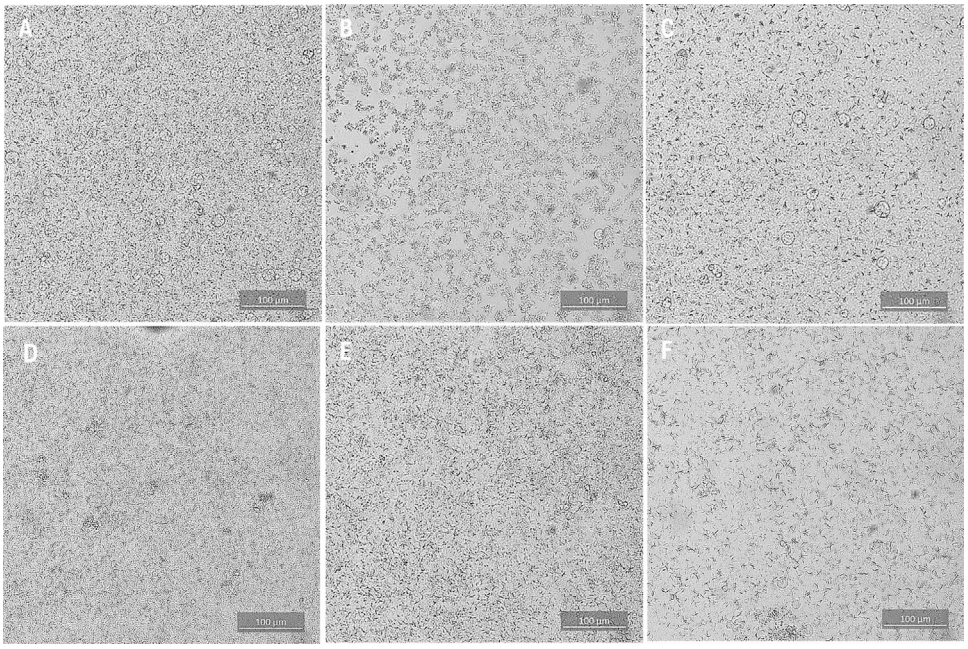

Figure 12. Images of 4% w/w BWX oleogels. A–C) Cooled at 10 °C min^{-1}, from left to right: stripped (A), untreated (B), and deteriorated (C), highest PC) canola oil. Bottom: cooled at 0.05 °C min^{-1} from left to right: D) stripped, E) untreated, and F) deteriorated, highest PC) canola oil. Scale bar: 100 µm.

cooled at 10 °C min^{-1} while the cooling rate was 0.05 °C min^{-1} for the images depicted at the bottom (D–F). The PC concentration increases from left to right from stripped to untreated to deteriorated (highest PC concentration). The figures mentioned above only show oleogels produced with canola oil since equivalent images were obtained utilizing sunflower oil.

In SFX oleogels cooled at 10 °C min^{-1}, the surface seems packed with the needle-like structures reported in numerous publications (Figure 10).[3,28,50,56,57] It should be mentioned that this shape is due to the 2D perspective since it was shown using scanning electron microscopy (SEM) that they are an interconnected network of platelets.[23] However, even though samples

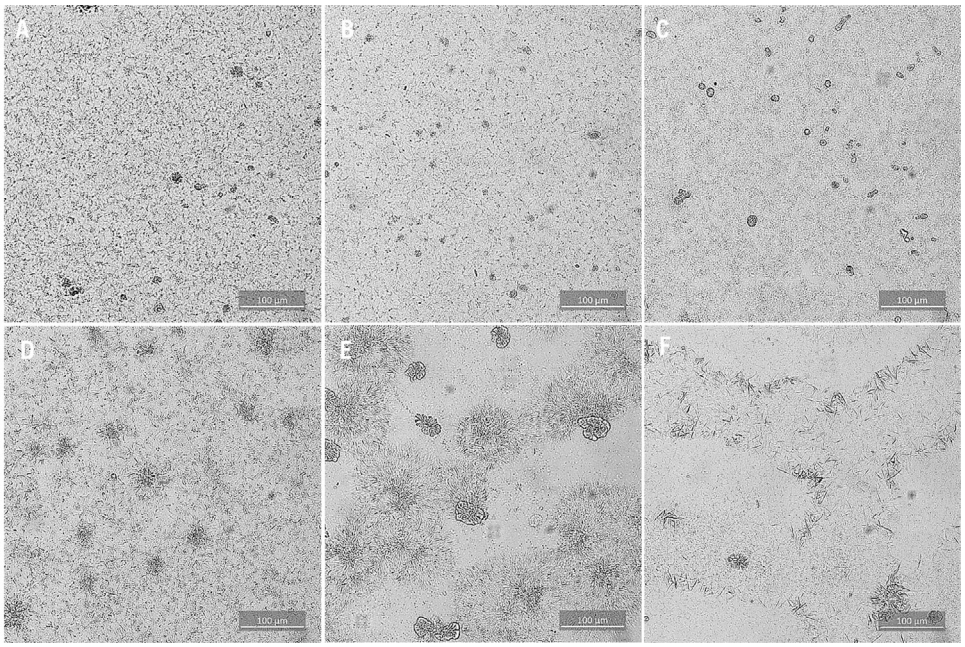

Figure 13. Images of 4% w/w CLX oleogels. A–C) Cooled at 10 K min^{-1}, from left to right: stripped (A), untreated (B), and deteriorated (C), highest PC) canola oil. Bottom: cooled at 0.05 K min^{-1} from left to right: D) stripped, E) untreated, and F) deteriorated, highest PC) canola oil. Scale bar: 100 µm.

were cooled rapidly, differences due to the presence and absence of PC can be seen. These modifications could be quantified well due to the good contrast between crystals and background. The crystal size was largest in samples with untreated (Figure 10B) canola oil and decreased in stripped (A) and deteriorated oil (C). Moreover, the fractal dimension was highest and the porosity lowest in samples comprising untreated oil. That indicates that a moderate level of minor oil components somewhat promotes the formation of a denser network that is relatively homogenous. Interestingly, the more ordered structure does not translate into an increased gel hardness (Figure 2). A similar effect has been reported for sterol/sterol ester oleogels.[35] However, this does not automatically result in firmer gels (see Section 3.3).

The effect of PCs is even more pronounced in samples cooled at 0.05 °C min^{-1}. In stripped oils (Figure 10D), needle-like structures turn into highly ordered crystal shards, which appear to grow 2D and look astonishingly similar to images of pure WE.[23] Hence, the low cooling rate promotes the crystallization into a highly ordered WE crystal that is largely absent in oils containing PC, especially at the highest PC level. Hence it is fair to assume that PC acts as a crystal modifier in SFX oleogels. Unfortunately, the shards were not detected sufficiently during image analysis due to poor contrast, resulting in the underevaluation of the crystal sizes. However, that indicates that the size of the crystalline building blocks must be very small.

RBX (Figure 11) produces significantly different crystal shapes than SFX, although their compositions appear quite similar at first sight (Table 3). In the literature, different shapes of wax crystals were reported in oleogels utilizing different oils. For example, in olive, canola, and peanut oil, RBX formed needle-shaped crystals similar to those observed in SFX oleogels.[3,29,57] However, more irregular-shaped crystals were observed in rice bran oil.[26,58] The effects appear to be related to minor wax, and potentially oil components since the bleaching of RBX resulted in different crystal shapes than those found in crude RBX.[52]

Additionally, the differences induced by variations of the cooling rate and polar components level appear even more distinct than in SFX samples (Figure 11). Knob-like structures can be seen in stripped oils at high cooling rates, while they appear elongated and cluster more in oils comprising PC. Moreover, other, more loosely organized crystalline structures can be seen in gels comprising untreated and deteriorated canola oil. The presence of these smaller structures might be connected to the tremendous increase in $\Delta G''$ observed during amplitude sweeps. Vice versa, the monocrystalline knobs observed in stripped oils do not form many movable fragments when gels are exposed to stress. However, this is very speculative.

Unfortunately, the clustered crystals were detected as single crystals during the crystal size determination, resulting in the largest crystal size and high deviations. However, in samples from stripped oils, crystals are more evenly distributed with less space between them, indicated by a higher fractional dimension and lower porosity. From visual observations, it is further suggested that the crystal size distribution is more homogenous. However, samples made with untreated and deteriorated oil at 10 °C min^{-1} were significantly harder, suggesting that the formation of distinct crystal types is beneficial in RBX oleogels. In line with that, gels cooled at 0.05 °C min^{-1} were considerably harder than those cooled at 10 °C min^{-1}. From Figure 11, bottom, it can be seen that RBX does not crystallize uniformly under these conditions (low supersaturation). The presence of large spherulitic crystal arrangements next to a finely distributed mesh of small crystals is difficult to interpret. The large crystals could be due to limited nucleation events followed by slow growth. If these nuclei result from homogeneous nucleation due to components with high melting points or emerge from heterogeneous

nucleation remains unresolved here. The size and density of the fine crystals appear to be modified in the presence of PC. The crystal sizes for 0.05 °C min^{-1} were significantly smaller than for samples gelled at 10 °C min^{-1}. That contradicts the assumptions made at the beginning of this chapter. However, it needs to be mentioned that the large crystals observed in slowly cooled samples were not taken into account for image analysis.

Figure 12 shows images of 4% w/w BWX oleogels. At first glance, a finely distributed network of very small crystals can be seen independently of the cooling rate and PC concentration. However, their distribution and porosity appear different. At high cooling rates, there is a very dense mesh of crystals. In line with that, the porosity is lowest and the fractal dimension highest, indicating a dense network with homogeneously distributed crystals. These structures appear looser and less dense in samples produced from untreated oils, with more free space between them. The size distribution in the sample with the highest PC did not confirm the visual observations, possibly due to a lack of contrast between crystals and background and low magnification. In samples cooled at 0.05 °C min^{-1}, the samples from stripped oil seem to be even finer than at 10 °C min^{-1}, with some larger, more ordered structures in between. In gels produced with untreated oil, a dense network of slightly bigger crystals can be seen, which is very homogenous, having a fractal dimension of 1.92. However, there due to larger crystals, there is more free space and thus higher porosity. At high PC levels, crystals are even larger (9.58 μm^2) and appear more ordered, leaving more free space between them (porosity 0.85). Moreover, the looser structures observed for slowly cooled samples comprising PC seem to relate to a lower gel hardness.

Finally, Figure 13 shows the samples produced with CLX at different cooling rates and concentrations of PC. Like BWX oleogels, a dense network of small crystals is formed by CLX when samples are cooled at 10 °C min^{-1} (Figure 13A-C). All three samples showed similar porosity and fractal dimension. However, in contrast to BWX, the crystals appear denser in gels produced with stripped oils, which is likely due to these samples' controlled crystallization of hentriacontane (C31). Nevertheless, the more delicate structures observed in oleogels comprising deteriorated (C) oil result in a considerable increase in hardness (see Figure 3).

A different picture emerges for gels produced using 0.05 °C min^{-1} (Figure 13D–F). Large and highly ordered structures can be seen, especially in stripped (D) and untreated oil (E), indicating a crystallization into separate crystalline structures similar to RBX. Fine crystals accompany them, homogeneously distributed in stripped oils (fractal dimension 1.94), leaving less free space between (porosity 0.63). In contrast, in untreated oils, these are partly attached to the crystals associated with hentriacontane. The gaps are filled with very small crystals, which cannot be seen in samples comprising stripped oils. In gels from deteriorated oil (F), these crystals make up most of the structure. Moreover, no highly ordered structures can be seen, indicating that mixed crystals' formation is promoted with PC. In line with SFX results, the gels with mixed crystals have a higher gel hardness than the highly ordered structures (see Figure 3).

Interestingly, in sunflower oil with the highest PC concentration, RBX crystals were modified and formed needle-like structures similar to those typical for SFX samples (Figure 10 and **Figure 14**). Thus, the data gathered once more illustrate the importance of minor oil components in oleogel technology. Their presence significantly affects the wax crystal appearance in edible oils, resulting in considerable modifications of the gels' macroscopic properties such as hardness and break-up behavior under stress. Furthermore, it was found that the effect of minor components is modified by the cooling rates applied to induced the sol-gel transition in wax oleogels.

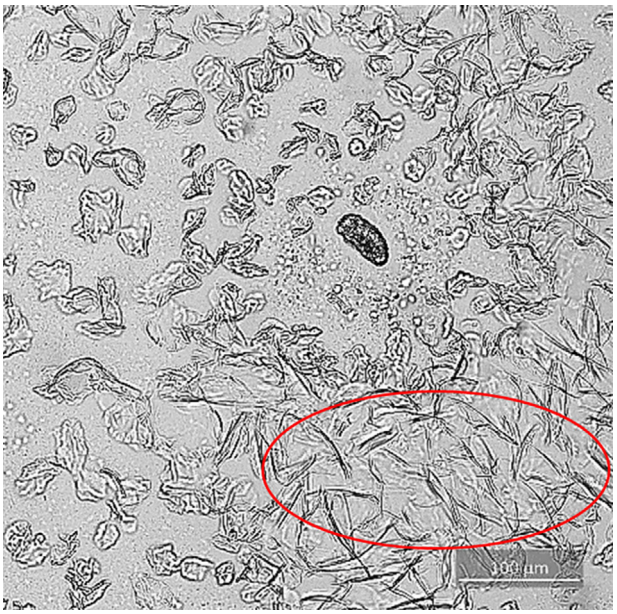

Figure 14. Image of a 4% w/w SFX oleogel produced with deteriorated sunflower oil, cooled at 10 K min^{-1}. Red circle indicates formation of structure similar to SFX oleogels.

4. Conclusion

The stripped oils serve as a reference for investigating the effects of polar components on wax oleogels. Significant effects of the cooling rate on several gel characteristics were shown. These modifications were particular for each wax type; hence no general conclusion could be formulated.

The gel characteristics of samples with PCs revealed significant differences in gel formation, enthalpy, rheological properties, and CGC compared to stripped oils. These were generally more pronounced at the slow cooling rate. Furthermore, the data on macroscopic hardness are complemented by rheological data, which in essence confirm that it is difficult to formulate any clear overarching relations of cooling rate and gel characteristics in the presence of PCs. Even more so, while macroscopic hardness is assessed to be reduced due to minor components, the rheological data indicate that the presence of PCs increases the resistance of the gel to deformation.

The thermal analysis (DSC) of oleogels based on stripped oils with different levels of structurants appeared to be very consistent and indicates that the applied cooling rate (10 °C min^{-1}) and stabilization procedures widely relate to solid-liquid equilibrium states. Building on this, the evolution of the kinetics of the crystallization and formation of kinetically induced mixed crystals at

different cooling rates and PC levels could be related to variations in cooling rate and serves as an explanation for specific phenomena encountered. The interpretations of the observations made on parameter variation are further supported by the light microscopical analysis of the samples. These indicate clearly that the effects of PCs and cooling rate are significant and specific for every wax.

The CGC increases with wax inhomogeneity and WE chain length difference (BWX > RBX > CLX > SFX). The wax concentration necessary to form a gel (CGC) is lower in the presence of polar components. That illustrates that the polar components contribute to the 3D network and support the solid matter's effectiveness in establishing a gel. However, these effects are less pronounced than in, for example, the sterol/sterol ester gels since, in this system, they strongly depend on hydrogen bonds.[49]

In conclusion, the data gathered illustrates that dissolved PCs significantly affect the gels' characteristics. The effects appear to be wax-type specific. However, it is consistently found that polar components increase the wax's solubility and support the formation of the gel itself. These two counteracting effects complicate the overall assessment and hinder any direct functional relation formulation.

To further address the topic, the authors suggest relating waxes' physical and chemical properties and their respective oleogels in standardized oils (depleted from minor components). Subsequently, the addition of relevant minor components could provide information about the gels' modifications regarding their functional groups.[21] To this end, XRD, the determination of FTIR spectra, and molecular modelling have proven to be powerful tools.[48,59,60]

Acknowledgements

Open access funding enabled and organized by Projekt DEAL.

Conflict of Interest

The authors declare no conflict of interest.

Data Availability Statement

The data that support the findings of this study are available from the corresponding author upon reasonable request.

Keywords

microscopy, minor oil components, oil structuring, oleogels, wax oleogels

Received: March 30, 2021
Revised: March 1, 2022
Published online: May 9, 2022

[1] C. D. Doan, Ph.D. Thesis, Ghent University, Ghent, Belgium **2017**.
[2] A. I. Blake, J. F. Toro-Vazquez, H. - S. Hwang, in *Edible Oleogels*, (Eds: A. Marangoni, N. Garti) Elseview, London, United Kingdom **2018**, p. 133.
[3] A. I. Blake, E. D. Co, A. G. Marangoni, *J. Am. Oil Chem. Soc.* **2014**, *91*, 885.
[4] A. A. Carelli, L. M. Frizzera, P. R. Forbito, G. H. Crapiste, *J. Am. Oil Chem. Soc.* **2002**, *79*, 763.
[5] L. S. K. Dassanayake, D. R. Kodali, S. Ueno, K. Sato, *J. Am. Oil Chem. Soc.* **2009**, *86*, 1163.
[6] J. Gómez-Estaca, A. M. Herrero, B. Herranz, M. D. Álvarez, F. Jiménez-Colmenero, S. Cofrades, *Food Hydrocolloids* **2019**, *87*, 960.
[7] H. - S. Hwang, S. Kim, M. Singh, J. K. Winkler-Moser, S. X. Liu, *J. Am. Oil Chem. Soc.* **2012**, *89*, 639.
[8] A. R. Patel, in *Alternative Routes to Oil Structuring* (Ed: A. R. Patel), Springer, Cham **2015**, pp. 15–27.
[9] A. F. Harron, M. J. Powell, A. Nunez, R. A. Moreau, *Ind. Crops Prod.* **2017**, *98*, 116.
[10] G. V. Buitimea-Cantúa, S. O. Serna-Saldívar, E. Pérez-Carrillo, T. J. Silva, D. Barrera-Arellano, N. E. Buitimea-Cantúa, *Grasas y Aceites* **2022**, *73*, 110267.
[11] S. R. Vali, Y. - H. Ju, T. N. B. Kaimal, Y. - T. Chern, *J. Am. Oil Chem. Soc.* **2005**, *82*, 57.
[12] C. D. Doan, I. Tavernier, P. K. Okuro, K. Dewettinck, *Innovative Food Sci. Emerging Technol.* **2018**, *45*, 42.
[13] A. Papadaki, N. Kopsahelis, D. M. G. Freire, I. Mandala, A. A. Koutinas, *Biomolecules* **2020**, *10*, 10.
[14] D. Johansson, B. Bergenståhl, *J. Am. Oil Chem. Soc.* **1992**, *69*, 705.
[15] D. Johansson, B. Bergenståhl, *J. Am. Oil Chem. Soc.* **1995**, *72*, 205.
[16] D. Johansson, B. Bergenståhl, *J. Am. Oil Chem. Soc.* **1992**, *69*, 728.
[17] D. Johansson, B. Bergenståhl, *J. Am. Oil Chem. Soc.* **1995**, *72*, 911.
[18] H. J. Ensikat, M. Boese, W. Mader, W. Barthlott, K. Koch, *Chem. Phys. Lipids* **2006**, *144*, 45.
[19] *Structure Function of Edible Fats*, (Ed: A. G. Marangoni), AOCS Press, Urbana, IL **2012**.
[20] F. G. Gandolfo, A. Bot, E. Flöter, *J. Am. Oil Chem. Soc.* **2004**, *81*, 1.
[21] M. Scharfe, D. Prange, E. Flöter, *J. Am. Oil Chem. Soc.* **2022**, *99*, 57.
[22] C. D. Doan, C. M. To, M. de Vrieze, F. Lynen, S. Danthine, A. Brown, K. Dewettinck, A. R. Patel, *Food Chem.* **2017**, *214*, 717.
[23] H. Brykczynski Wax-based oleogels- characterization and re—engineering of waxes. Master Thesis, Technical University Berlin, Berlin 2021.
[24] B. T. Iyengar, H. Schlenk, *Lipids* **1969**, *4*, 28.
[25] G. Avendaño-Vásquez, A. De la Peña-Gil, M. E. Charó-Alvarado, M. A. Charó-Alonso, J. F. Toro-Vazquez, *Front. Sustain. Food Syst.* **2020**, *4*, 1.
[26] C. D. Doan, D. van de Walle, K. Dewettinck, A. R. Patel, *J. Am. Oil Chem. Soc.* **2015**, *92*, 801.
[27] Z. Meng, K. Qi, Y. Guo, Y. Wang, Y. Liu, *Food Chem.* **2018**, *246*, 137.
[28] S. Martini, C. Y. Tan, S. Jana, *J. Food Sci.* **2015**, *80*, C989 .
[29] L. S. K. Dassanayake, D. R. Kodali, S. Ueno, K. Sato, *J. Oleo Sci.* **2012**, *61*, 1.
[30] A. Lopez-Martínez, M. A. Charó-Alonso, A. G. Marangoni, J. F. Toro-Vazquez, *Food Res. Int.* **2015**, *72*, 37.
[31] A. J. Gravelle, M. Davidovich-Pinhas, A. K. Zetzl, S. Barbut, A. G. Marangoni, *Carbohydr. Polym.* **2016**, *135*, 169.
[32] A. Aliasl khiabani, M. Tabibiazar, L. Roufegarinejad, H. Hamishehkar, A. Alizadeh, *Food Chem.* **2020**, *333*, 127446.
[33] A. Aliasl Khiabani, M. Tabibiazar, L. Roufegarinejad, H. Hamishehkar, A. Alizadeh, *J. Am. Oil Chem. Soc.* **2018**, *95*, 797.
[34] J. F. Toro-Vazquez, M. Alonzo-Macias, E. Dibildox-Alvarado, M. A. Charó-Alonso, *Food Biophys.* **2009**, *4*, 199.
[35] M. Scharfe, Y. Ahmane, J. Seilert, J. Keim, E. Flöter, *Eur. J. Lipid Sci. Technol.* **2019**, *121*, 1800487.
[36] M. Scharfe, *On the Importance of Minor Components and Oil Properties for Sterol/Sterol Ester Strength*, Sevilla, Spain **2019**.
[37] V. Giacintucci, C. D. Di Mattia, G. Sacchetti, F. Flamminii, A. J. Gravelle, B. Baylis, J. R. Dutcher, A. G. Marangoni, P. Pittia, *Food Hydrocolloids* **2018**, *84*, 508.

[38] H. - S. Hwang, J. D. Gillman, J. K. Winkler-Moser, S. Kim, M. Singh, J. A. Byars, R. L. Evangelista, *J. Am. Oil Chem. Soc.* **2018**, *95*, 557.
[39] J. A. Morales-Rueda, E. Dibildox-Alvarado, M. A. Charó-Alonso, R. G. Weiss, J. F. Toro-Vazquez, *Eur. J. Lipid Sci. Technol.* **2009**, *111*, 207.
[40] A. - M. Lampi, A. Kamal-Eldin, *J. Am. Oil Chem. Soc.* **1998**, *75*, 1699.
[41] A. Mariod, B. Matthäus, I. H. Hussein, *J. Am. Oil Chem. Soc.* **2011**, *88*, 603.
[42] M. Scharfe, D. Prange, E. Flöter, *J. Am. Oil Chem. Soc.* **2022**, *99*, 43.
[43] International Organization for Standardization, Animal and vegetable fats and oils- determination of content of polar compounds: Revised Version 2018 2002, International Organization for Standardization.
[44] Deutsches Institu for Normung e.V., DIN 53019-4:2016-10, Rheometrie_- Messung von Fließeigenschaften mit Rotationsrheometern_- Teil_4: Oszillationsrheologie, Beuth Verlag GmbH, Berlin. doi: 10.31030/2560192 .
[45] T. G. Mezger, *Das Rheologie Handbuch: Für Anwender von Rotations- und Oszillations-Rheometern*, Vincentz Network, Hannover **2016**.
[46] T. Wettlaufer, B. Hetzer, E. Flöter, *Eur. J. Lipid Sci. Technol.* **2021**, *123*, 2000345.
[47] I. Tavernier, Ph.D. Thesis, Ghent University, Ghent, Belgium **2018**.
[48] A. B. Matheson, V. Koutsos, G. Dalkas, S. Euston, P. Clegg, *Langmuir* **2017**, *33*, 4537.
[49] G. Dalkas, A. B. Matheson, H. Vass, A. Gromov, G. O. Lloyd, V. Koutsos, P. S. Clegg, S. R. Euston, *Langmuir* **2018**, *34*, 8629.
[50] A. R. Patel, M. Babaahmadi, A. Lesaffer, K. Dewettinck, *J. Agric. Food Chem.* **2015**, *63*, 4862.
[51] H. - S. Hwang, M. Singh, J. K. Winkler-Moser, E. L. Bakota, S. X. Liu, *J. Food Sci.* **2014**, *79*, C1926 .
[52] S. Pandolsook, S. Kupongsak, *J. Food Eng.* **2017**, *214*, 182.
[53] J. C. B. Rocha, J. D. Lopes, M. C. N. Mascarenhas, D. B. Arellano, L. M. R. Guerreiro, R. L. da Cunha, *Food Res. Int.* **2013**, *50*, 318.
[54] A. G. Marangoni, *Edible Oleogels: Structure and Health Implications*, Elsevier, Cambridge MA **2018**.
[55] A. I. Blake, *The Microstructure and Physical Properties of Plant-Based Waxes and their Relationship to the Oil Binding Capacity of Wax Oleogels*, Dissertation, Guelph **2015**.
[56] H. - S. Hwang, S. Kim, K. O. Evans, C. Koga, Y. Lee, *Food Struct.* **2015**, *5*, 10.
[57] A. I. Blake, A. G. Marangoni, *Food Biophys.* **2015**, *10*, 403.
[58] I. Tavernier, C. D. Doan, D. van de Walle, S. Danthine, T. Rimaux, K. Dewettinck, *RSC Adv.* **2017**, *7*, 12113.
[59] A. Matheson, G. Dalkas, R. Mears, S. R. Euston, P. S. Clegg, *Soft Matter* **2018**, *14*, 2044.
[60] E. Yılmaz, M. Öğütcü, *J. Am. Oil Chem. Soc.* **2014**, *91*, 1007.